NSF/ENG-85071

PB87-148177

PMFSEL REPORT NO. 85-3
DECEMBER 1985

BEHAVIOR OF STRENGTHENED AND REPAIRED REINFORCED CONCRETE COLUMNS UNDER CYCLIC DEFORMATIONS

By

Bart J. Bett
Richard E. Klingner
James O. Jirsa

Report on a Research Project
Sponsored by
National Science Foundation
Grant No. CEE-8201205

PHIL M. FERGUSON STRUCTURAL ENGINEERING LABORATORY
Department of Civil Engineering / Bureau of Engineering Research
The University of Texas at Austin

REPRODUCED BY
U.S. DEPARTMENT OF COMMERCE
NATIONAL TECHNICAL
INFORMATION SERVICE
SPRINGFIELD, VA 22161

BEHAVIOR OF STRENGTHENED AND REPAIRED REINFORCED CONCRETE COLUMNS UNDER CYCLIC DEFORMATIONS

by

Bart J. Bett

Richard E. Klingner

and

James O. Jirsa

Report on a Research Project
Sponsored by
National Science Foundation
Grant No. CEE-8201205

Phil M. Ferguson Structural Engineering Laboratory
Department of Civil Engineering
BUREAU OF ENGINEERING RESEARCH
THE UNIVERSITY OF TEXAS AT AUSTIN

December 1985

The contents of this report reflect the views of the authors who are responsible for the facts and accuracy of the data presented herein. The contents do not necessarily reflect the view or policies of the National Science Foundation. This report does not constitute a standard, specification, or regulation.

ACKNOWLEDGMENTS

The research reported was conducted as part of the Master of Science program of Bart J. Bett under the direction of Dr. R. E. Klingner. The advice and guidance of Dr. R. L. Carrasquillo of The University of Texas and Loring Wyllie, Jr., Chris Poland, and Roy Moreno of H. J. Degenkolb Associates, Inc., San Francisco, California were most helpful throughout the test program and are gratefully acknowledged.

This project was funded under National Science Foundation Grant No. CEE-8201205. H. J. Degenkolb Associates, Inc. is participating in the project under a separate NSF Grant (CEE-8201187).

The experimental work was conducted in the Ferguson Structural Engineering Laboratory at Balcones Research Center of The University of Texas at Austin. The technical and administrative staff of the Laboratory provided the necessary support for the project and without their cooperation and dedication the project could not have been done. The many graduate assistants who helped with various tasks also added much to the success of the research.

CONTENTS

CONTENTS (continued)

TABLES

FIGURES

Figure		Page

Figure		Page

CHAPTER 1

INTRODUCTION

1.1 Background

Reinforced concrete buildings in seismic zones are repaired or strengthened for three reasons: 1) to repair earthquake damage and obtain improved performance during future events; 2) to comply with local building codes and regulations when the building's use is changed; and 3) to satisfy the building owner's concern for the safety of the occupants and protection of his financial investment.

The existing building must be thoroughly analyzed to determine the strengths and weaknesses of the original lateral force-resisting system, considering the building's functions and aesthetics. Strengthening schemes may involve the use of materials different from those of the original structure, and the interaction of those materials must be understood. The scheme selected must not create new areas of weakness, and must be economically feasible.

The need for information on the repair and strengthening of reinforced concrete structures is apparent. Several National Science Foundation- sponsored workshops on this topic have been held in the United States, and a number of U.S. research institutions (Portland Cement Association, University of Michigan, University of California-Berkeley) have studied repair techniques [1,2]. Repair and strengthening problems have received more attention in Japan [3,4]. Because experimental work in the area of repair and strengthening is very complex and expensive, most studies have involved small scale specimens. In addition, there has been little dialogue between researchers and designers who must incorporate research results into practice. These two concerns are addressed in the overall research program discussed in Chapter 2.

1.2 Objectives and Scope

The objective of this study was to evaluate several repair and strengthening techniques for reinforced concrete short columns. Short columns under constant axial compression were subjected to reversed cyclic deformations. Two columns were strengthened before testing, and one column was repaired after testing. Individual column test results were compared. Repair and strengthening techniques were evaluated in terms of strength, stiffness, and damage repair.

1.3 Short Columns in Structures

Field reports following various damaging earthquakes indicate that columns are vulnerable structural elements, particularly if they fail in shear. Shear-dominated behavior is most common in columns having shear-span depth (a/d) ratios less than 2.5 [5,6,7,8]. Short columns exist in structural systems either as part of the original design, or as the result of structural or architectural changes made during the life of the structure. Members originally designed as short columns can behave satisfactorily under lateral loads if designed for sufficient shear resistance. However, short (or "captive") columns are sometimes produced unintentionally [8,9] when clear column height is reduced by stiff elements that restrict the lateral deformation of the column over a portion of its length (Fig. 1.1). This change in length is important because the applied shear and moment on a column are related by its length, as shown in Fig. 1.2. The original column may have been properly designed to develop its flexural capacity before failing in shear. Due to the reduction in length, the captive column will often fail in shear before developing its flexural capacity. Post-earthquake structural investigations report many failures of captive columns restrained by structural or non-structural elements (Fig. 1.3).

1.4 Short-Column Repair/Strengthening Techniques

Severe seismic loading of columns with small shear-span/depth (a/d) ratios and widely-spaced transverse reinforcement generally results in shear-dominated failure, leading to structural collapse by the formation of a single- story sidesway mechanism. While this can be prevented by increasing column shear capacity, it must be done economically, and without large increases in flexural capacity, which would increase applied shears. Figure 1.4 illustrates four methods now available for increasing the shear capacity of a vulnerable column: 1) encase it with rectangular or circular steel sections; 2) encase it with steel straps; 3) confine it by using welded wire fabric; and 4) confine it by adding spliced ties. A jacket of shotcrete or cement grout is then applied to protect the added steel and make it act integrally with the original column.

Jacketing can increase the shear resistance of the column, but may adversely affect the building's seismic resistance: decreased (a/d) ratio and increased moment capacity make shear-dominated column failure more likely; increased column stiffness decreases the building's fundamental period and increases seismic-induced lateral forces. However, jacketing of the original column is still beneficial; 1) due to increased confinement, column shear performance is adequate even at lower (a/d) ratios; 2) judicious selection and placement of jacket longitudinal steel minimizes increases in column

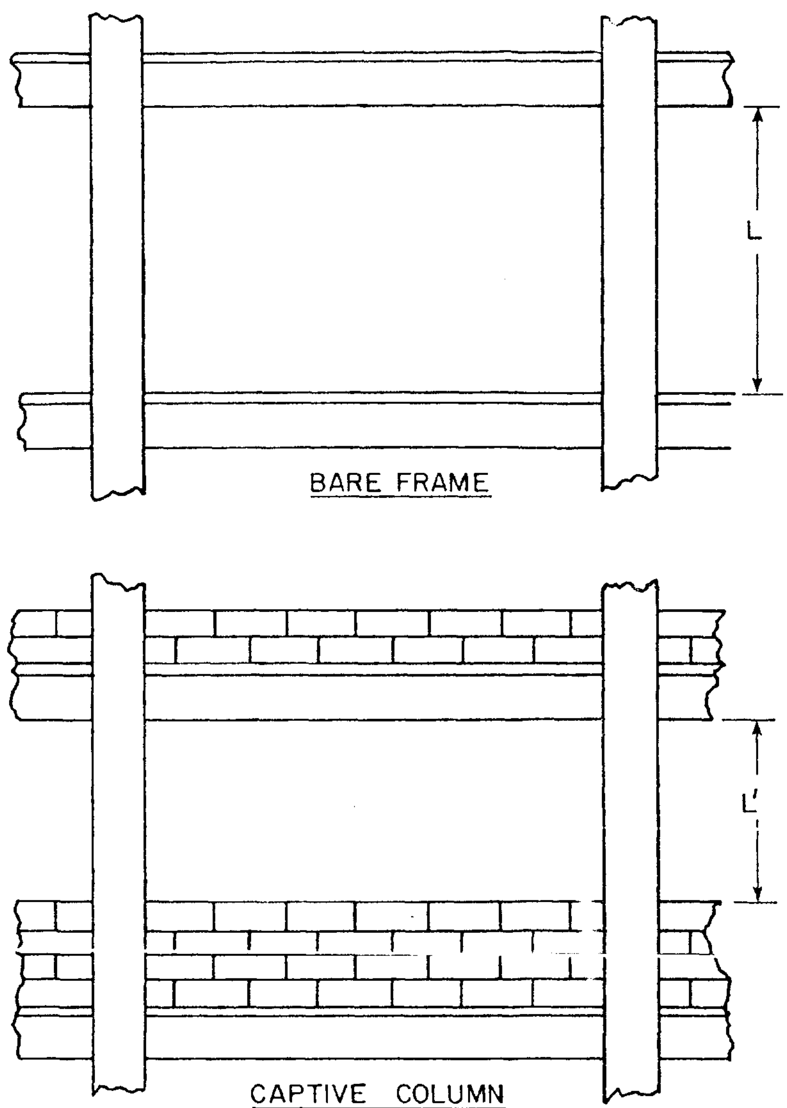

Fig. 1.1 Captive column concept

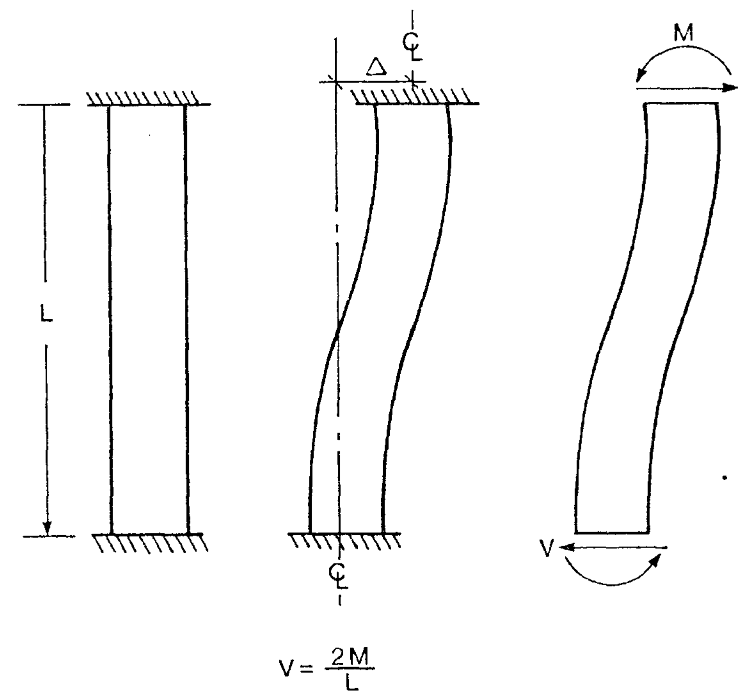

Fig. 1.2 Relation between end shears and moments in a column subjected to sidesway

Fig. 1.3 Failed columns at Misawa Commercial High School, Tokachi-Oki earthquake, Japan, 1968.

Reproduced from best available copy.

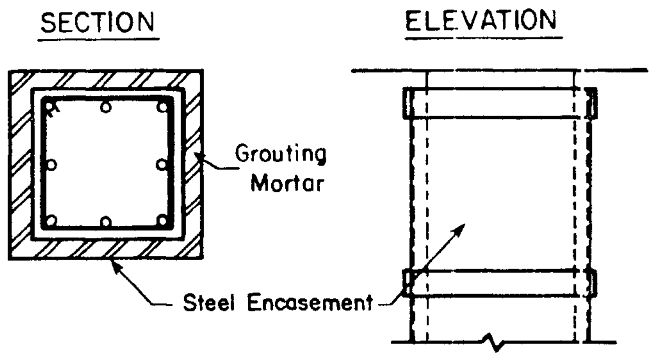

a) strengthening by steel encasement

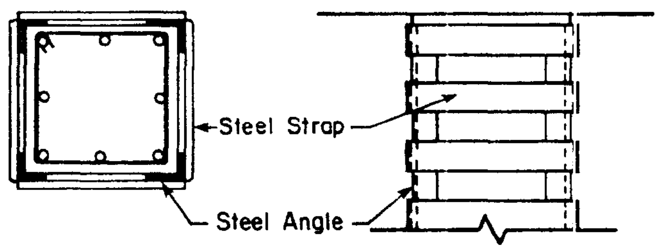

b) strengthening by steel straps and angles

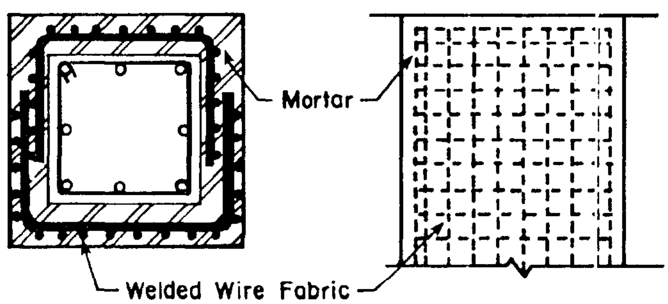

c) strengthening by welded wire fabric

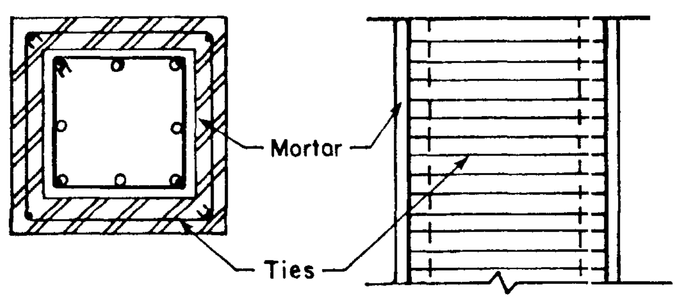

d) strengthening by closely-spaced ties

Fig. 1.4 Techniques to increase shear capacity [13].

flexural capacity; and 3) increased column shear capacity offsets increases in seismic-induced lateral forces.

Retrofitting techniques can be evaluated experimentally in terms of strength and stiffness. The behavior of a column, initially tested, repaired and strengthened, and then retested, can be compared to the behavior of initially strengthened columns, and a correlation developed between retrofitting technique and performance.

CHAPTER 2

EXPERIMENTAL PROGRAM

2.1 Introduction

The purpose of this study was to evaluate several repair and strengthening techniques for reinforced concrete short columns. Three test specimens were constructed using normal weight concrete and Gr. 60 reinforcement. One specimen was tested in its original form, repaired, strengthened, and retested. The remaining two specimens were strengthened prior to testing. The specimens were numbered sequentially (1-1, 1-2, 1-3) and the repaired specimen was designated by 1-1R. In each test, constant axial compression and numerous cycles of reversed lateral deformations were applied to the specimen. The primary objective of this test program was to study the effect of different strengthening or repair techniques on the strength and response characteristics of reinforced concrete short columns. In this chapter, the experimental program will be discussed. Much of the information is summarized in Table 2.1.

2.2 Overall Research Program

This investigation was part of a larger study of the behavior of reinforced concrete frame systems subjected to cyclic lateral deformations. The overall research program was devoted to evaluation of various repair and strengthening techniques for R/C frame elements. The study reported herein deals only with short columns.

In the overall research program the capabilities of a university research laboratory and a structural engineering design firm were combined. Repair and strengthening is a specialized area in which professional experience is extremely important. Design requirements for strengthening techniques and details are not as codified as are requirements for original construction. Second, experiments were conducted using nearly full-scale specimens fabricated especially for studying repair and strengthening procedures, and not as an adjunct to a study with other primary objectives. The success of most repair techniques lies in the details utilized, and scale effects may be important.

2.3 Original Test Specimen (1-1)

2.3.1 Design Requirements. The objective of the project was to study the behavior of a reinforced concrete column that would fail in shear if it were not strengthened. To avoid the cost of designing

TABLE 2.1 Test Program Summary

Test No.	Specimen No.	Column Cross Section	Test Description
1	1-1	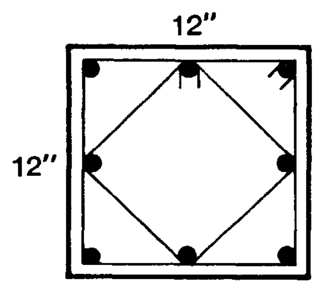 Long. steel: #6's Ties: 6mm @ 8" Identical 12" x 12" cores used for all specimens.	Description: original specimen Test: reversed unidirectional loading Deflection limit: 2% drift
2	1-2	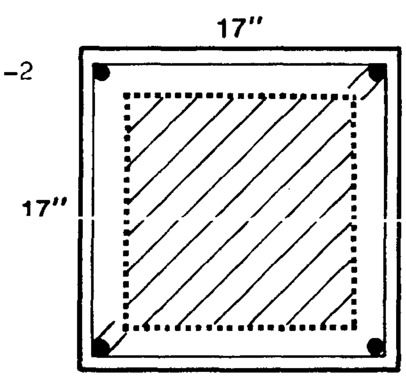 Long. steel: #3's Ties: 6mm @ 2-1/2" 2-1/2" shotcrete shell	Description: sandblast, add 4-#3 longitudinal bars and 6mm ties at 2-1/2". Shotcrete to 17" x 17". Test: reversed unidirectional loading. Deflection limit: 2.5% drift

TABLE 2.1 Test Program Summary (continued)

Test No.	Specimen No.		Column Cross Section	Test Description
3	1-3	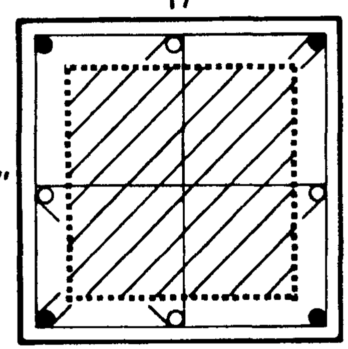	Long: #3's, #6's Ties: 6mm @ 2-1/2" Crossties: #3's @ 9" 2-1/2" shotcrete shell	Description: sandblast, add 4-#3 corner bars and 4-#6 midface bars. Anchor midface bars w/#3 crossties, secured with epoxy. 6mm ties @ 2-1/2". Shotcrete to 17" x 17". Test: reversed unidirectional loading. Deflection limit: 2.5% drift.
4	1-1R	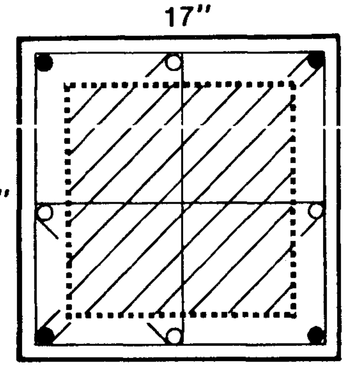	Long: #3's, #6's Ties: 6mm @ 2-1/2" Crossties: #3's @ 9" 2-1/2" shotcrete shell	Description: Remove all loose cover Add 4-#3 corner bars and 4-#6 midface bars. Anchor midface bars w/#3 crossties, secured with epoxy. 6mm ties @ 2-1/2". Shotcrete to 17" x 17". Test: reversed unidirectional loading. Deflection limit: 2.5% drift.

and constructing a new test frame, it was decided to use short column specimens of the same size as those studied in previous test programs [5,6,7,8,9]. The test specimen selected was a short column framing into enlarged end blocks, which provided both for attachment of the specimen to the test frame and for anchorage of the longitudinal column reinforcement.

The prototype short column was designed as an 18-in. (45.7 cm) square section meeting the column design provisions of ACI 318-63 [16], particularly Section 806 and Chapter 19. It was 4.5 ft (1.37 cm) high, and reinforced with eight #9 longitudinal bars (P_g = 0.025) and two sets of #3 ties at 12 in. Cover was 1-1/2 in. Transverse reinforcement spacing and details were selected as typical for structures designed for seismic regions of the U.S. during the late 1950's and early 1960's. Columns of such structures usually had transverse reinforcement which would be insufficient by current standards, resulting in shear-dominated behavior under severe lateral loads.

Column loads in the structures mentioned above vary widely. Based on actual load data [14], typical compressive stresses ranged from about 350 psi to 550 psi, with an average of about 450 psi. The axial load required to develop an average compressive stress of 450 psi on the prototype 18-in. square column is about 146 kips.

To reduce fabrication and testing costs, yet permit the use of commercially available deformed reinforcement, the test specimens were constructed to two-thirds scale. Analyses indicated that the previously used connection details between the frame and a strengthened specimen would be inadequate. Those details were subsequently modified as described in Chapter 3.

2.3.2 Details of Specimen. Details of the original test specimen are shown in Fig. 2.1. The two-thirds scale model was a 12-in. (30.5 cm) square section, 3.0 ft (0.92 m) in height, containing eight #6 longitudinal bars, sets of special 6 mm deformed ties at 8 in., and 1 in. cover.

2.3.3 Calculated Strengths. The test specimen's theoretical moment and shear capacities were calculated using the computer program RCCOLA, developed for inelastic flexural analysis of reinforced concrete sections [15]. Although moment capacity can be estimated fairly accurately, shear capacity is more difficult to predict. The program used an empirical relationship Eq. 2.1 based on University of Texas short column test results [23].

$$V_{nr} = \left(11 - 3\frac{a}{d^*}\right) A_c \sqrt{f'_c} + \frac{0.2\ N}{\frac{a}{d^*}}$$

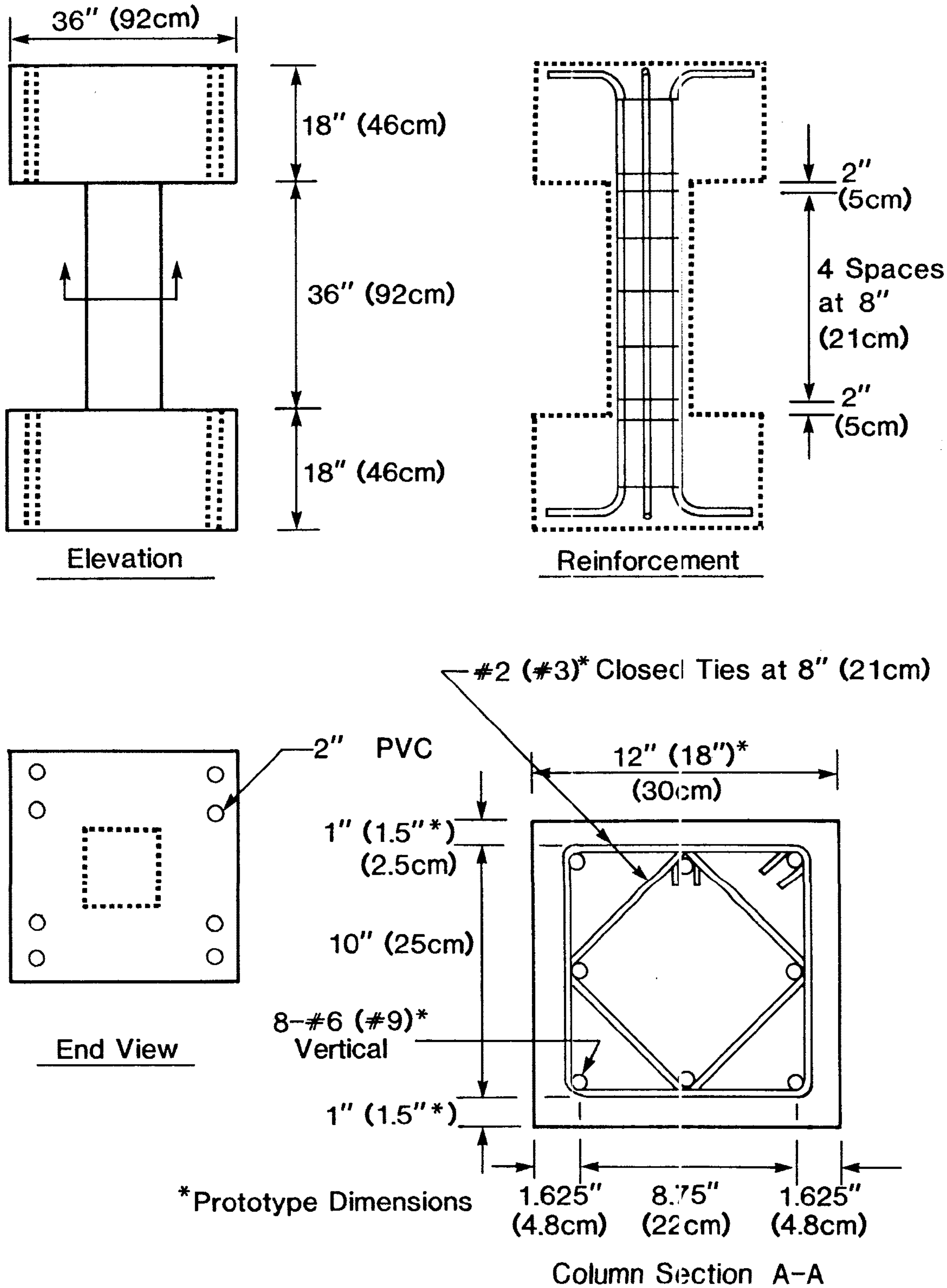

Fig. 2.1 Details of original specimen

$$\frac{0.2\,N}{\frac{a}{d^*}} \leq \frac{160\,A_g}{\frac{a}{d^*}}$$

$$1 \leq \frac{a}{d^*} \leq 2.5 \tag{2.1}$$

Using the above shear resistance, and the statical relations between shear end moments in a column subjected to sidesway (Fig. 1.2), a diagram of moment capacity as governed by shear was produced (Fig. 2.2). Capacities are shown for both the initial (entire) and confined cross sections. The shear capacity plot indicates the level of end moment required to generate the column's shear capacity at any axial load. Inspection of Fig. 2.2 reveals that the shear capacity curve becomes vertical for large axial loads. This conservative limit was due to the absence of test results for large axial loads. Neglecting the beneficial effects of axial compressive load on a column's shear capacity may be appropriate in the analysis of columns subjected to earthquakes. It is entirely possible that during a severe seismic event, the effect of overturning or vertical accelerations may reduce the level of axial compression significantly. Considering a 12 in. square column subjected to 450 psi compression (64.8 kips), the predicted end moment corresponding to flexural failure of the initial section is about 1150 in.-kips, and that corresponding to shear failure about 720 in.-kips. Based on the analytical model of Fig. 1.2, the corresponding lateral capacities are 64 kips (flexure) and 40 kips (shear). The original column could therefore be expected to fail in shear.

2.3.4 Specimen Fabrication. Dimensions of the end block were based on the requirements for attaching the test specimen to the test frame and for anchoring the longitudinal column reinforcement. Details of the end block reinforcement are shown in Fig. 2.3.

To simplify formwork, specimens were cast in two stages. First, the bottom end block was cast with the column and top block formwork already in place. Four days later the column and top end block were cast. This casting sequence produced a cold joint at the bottom of the column, and is similar to that used in reinforced concrete buildings. Figure 2.4 illustrates the specimen formwork.

2.4 Material Characteristics of Original Test Specimen

2.4.1 Concrete. Ready-mixed concrete was obtained from a local supplier, with the mix proportions, as shown in Table 2.2.

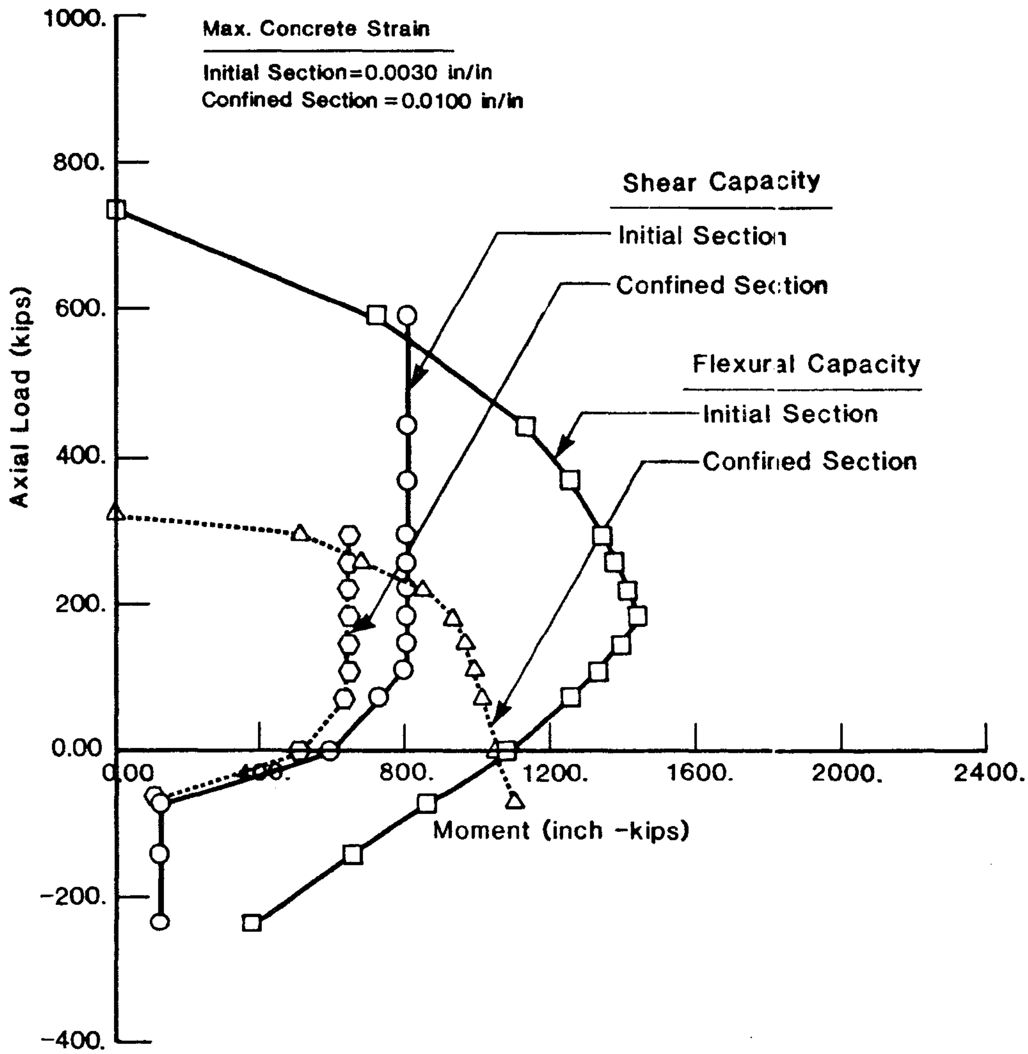

Fig. 2.2 Shear capacity-interaction diagram (original specimen)

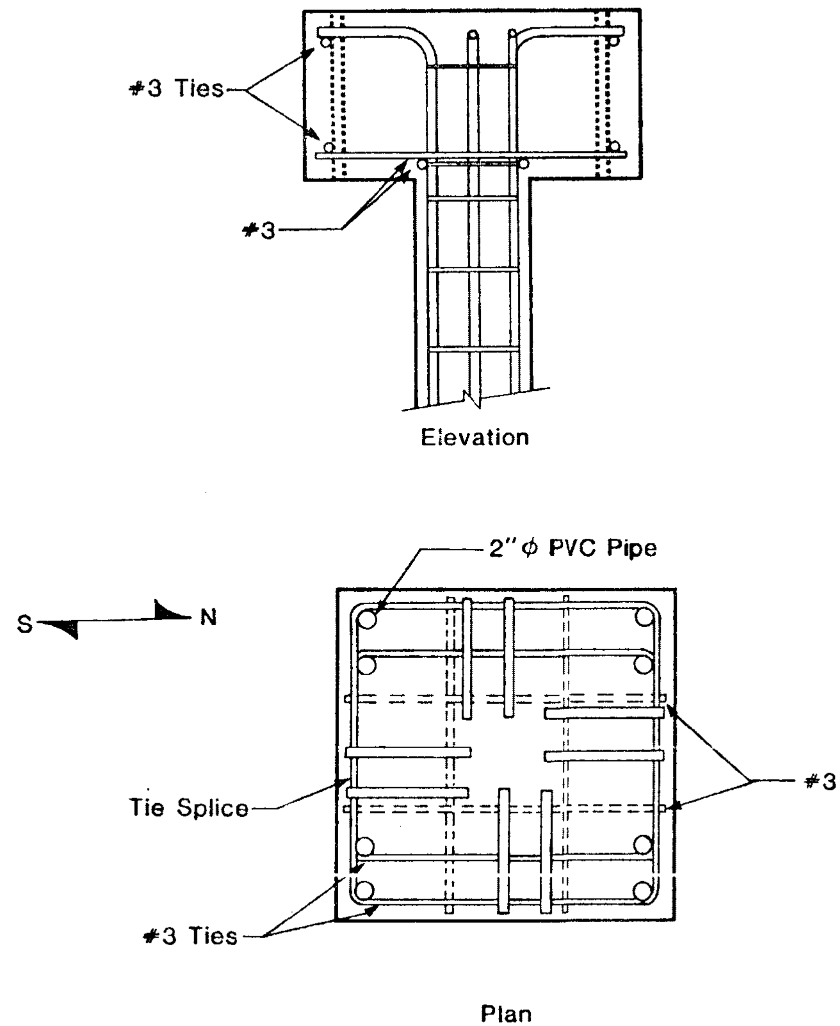

Fig. 2.3 Details of end block reinforcement

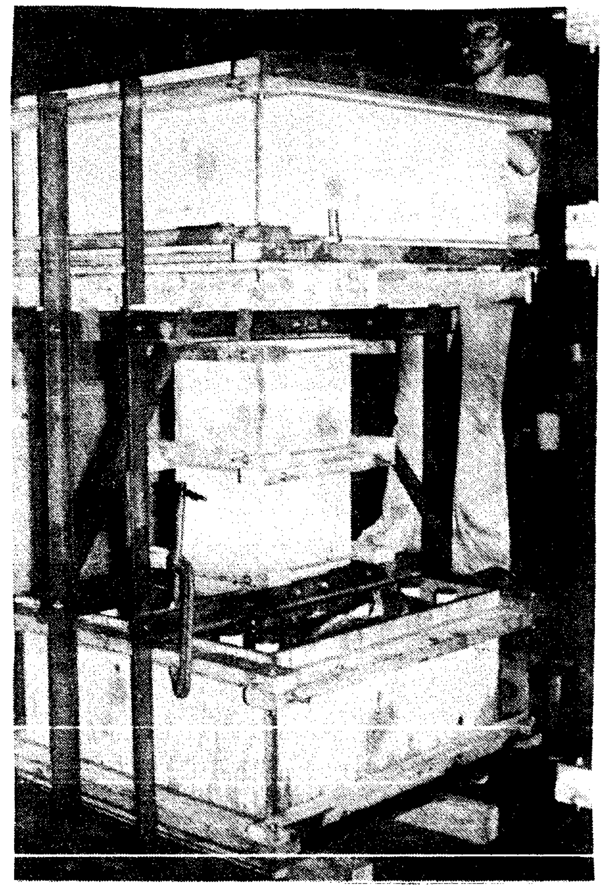

Fig. 2.4 Construction of formwork

TABLE 2.2 Column Concrete Strength

Concrete Mix Design (4000 psi) Proportions of 1 yd^3		Concrete Properties	Age (days)	Compressive Strength, f'_c (psi)
Water	210 lb		28	3831
Cement (5 sacks)	470 lb			
Fine aggregate	1530 lb	Test 1-1	57	4333
Coarse aggregate (5/8 in.)	1830 lb			
Trisene L (retarding admixture)	15 oz	Test 1-2	147	4399
(w/c = 0.45 by weight)		Test 1-1	204	4627

TABLE 2.3 Steel Properties (Original Column)

Bar Size	f_y (ksi)	E (ksi)		E_{sth} (ksi)	f_u (ksi)	
#6	67	25463	0.0079	1344	112	0.1445
6mm	60*	26625	0.00265	870	88	0.0975

* 0.2% offset

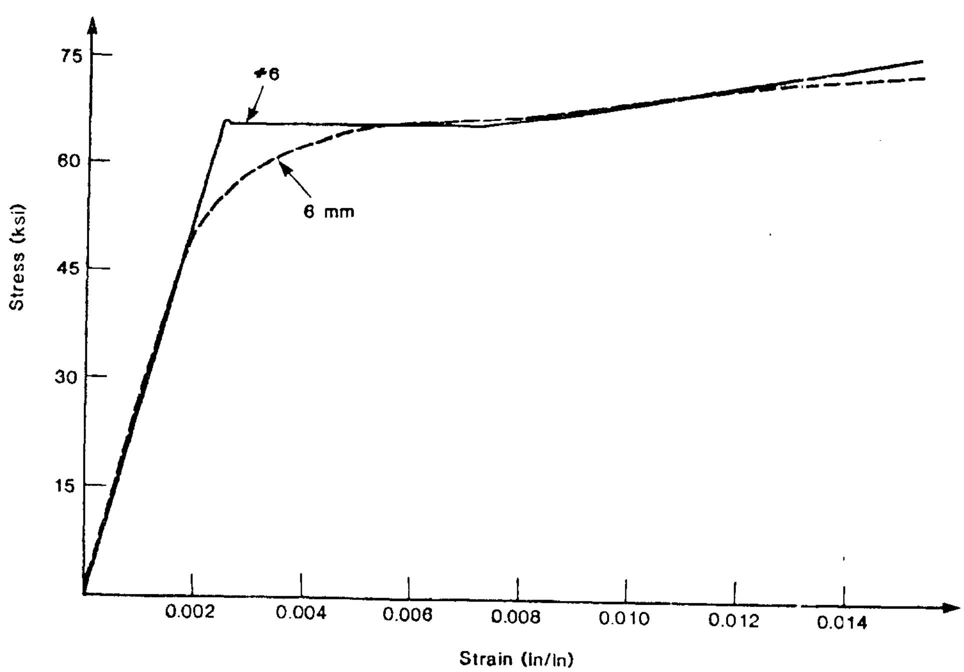

Fig. 2.5 Stress-strain curve for original specimen steel reinforcement

The aggregate was Colorado River sand and gravel. Because of congestion of reinforcement, a relatively high slump was necessary to ensure proper placement of concrete. The concrete was ordered with a slump less than the desired 7 in., and water was added on site to achieve the required slump. Twelve control cylinders were cast and cured with the specimens. All three specimens were cast in the same operation, and moist-cured under polyethylene sheets for seven days prior to stripping the forms.

Three control cylinders were capped and tested at 28 days, and at the conclusion of the first, second, and fourth tests. Table 2.2 summarizes the results of the cylinder tests.

2.4.2 Reinforcement. Number 6 deformed reinforcement (ASTM A-615 Gr. 60) was used for the longitudinal steel, and 6 mm deformed reinforcement for the transverse steel. The 6 mm deformed bars were fabricated in Sweden and obtained through the Portland Cement Association Laboratories. Mechanical characteristics of reinforcement are shown in Table 2.3, and typical stress-strain curves in Fig. 2.5.

2.5 Strengthened and Repaired Specimens

2.5.1 Strengthening Technique (Specimens 1-2, 1-3). Strengthening involved encasing the original column with a shotcrete jacket reinforced with closely-spaced transverse steel. Additional longitudinal steel was placed at each corner of the jacket to support the transverse steel. Details of the strengthening technique for each specimen will be described in subsequent sections.

2.5.2 Repair Technique (Specimen 1-1R). The repair technique consisted of two operations. First, all loose cover was removed with a chipping hammer, exposing the longitudinal steel. Holes were then drilled through the columns, and crossties used to anchor additional longitudinal steel were inserted and cemented with epoxy. Second, closely-spaced ties were placed around the column core, and it was encased with shotcrete. Details of the repair technique will be shown later.

2.6 Strengthened Specimen 1-2

2.6.1 Details. The strengthening technique used for Specimen 1-2 consisted of a shotcrete jacket reinforced as shown in Fig. 2.6.

2.6.2 Calculated Strengths. Theoretical moment and shear capacities, calculated as described previously [15], are shown in Fig. 2.7. Inspection of Fig. 2.7 reveals that for a 64.8 kip (224 psi) axial load, the end moment corresponding to flexural capacity is about

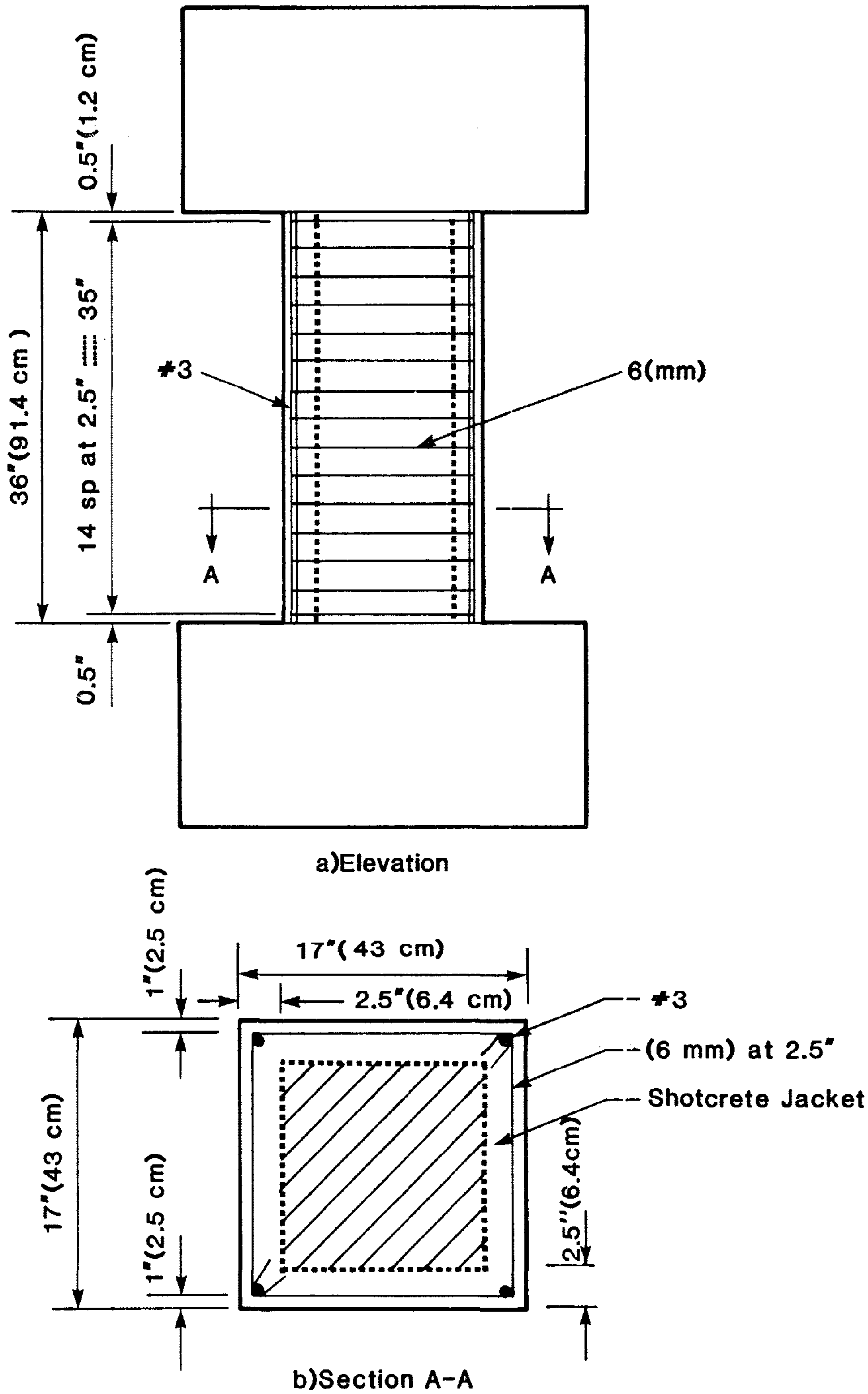

Fig. 2.6 Details of Specimen 1-2.

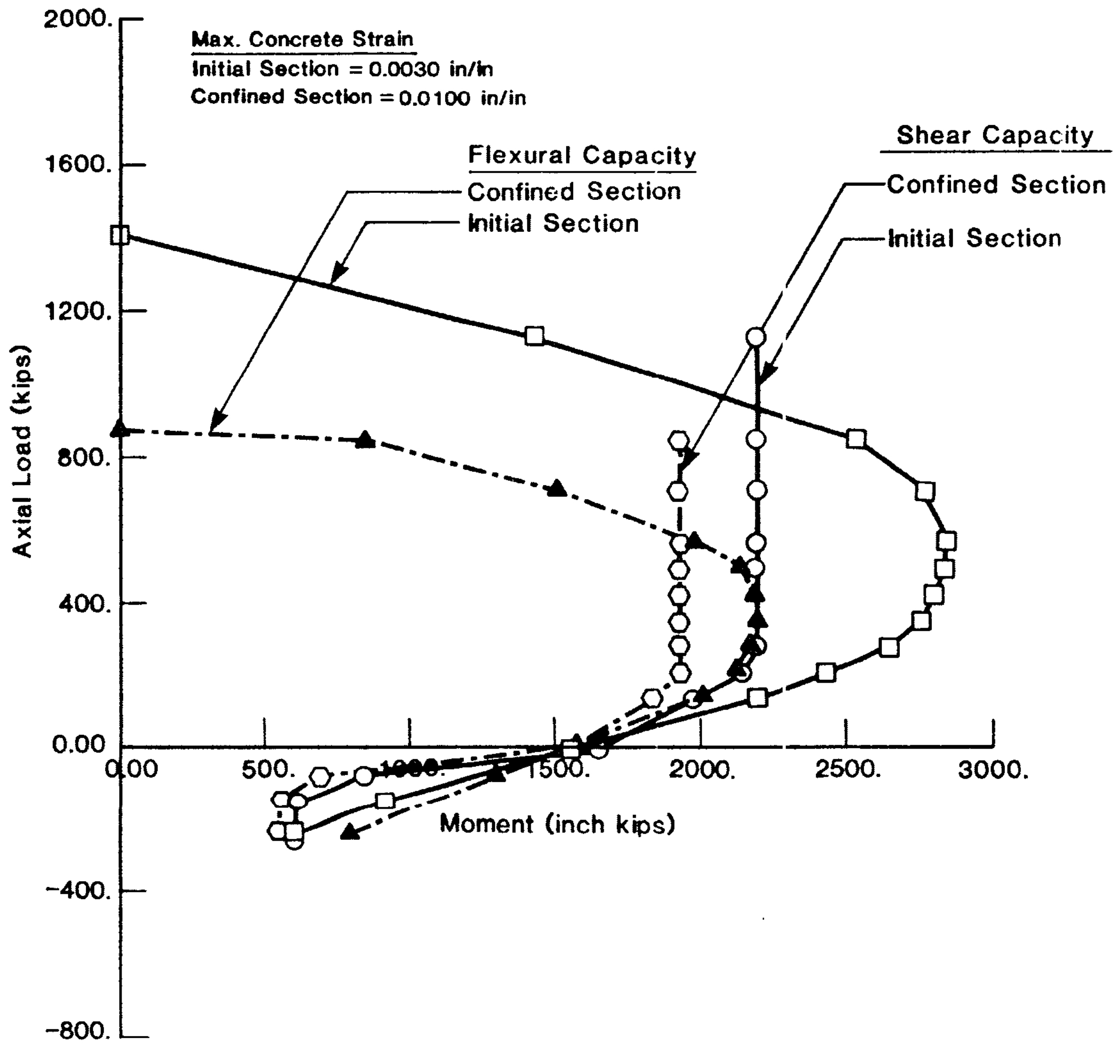

Fig. 2.7 Shear capacity-interaction diagram (Specimens 1-2, 1-3).

1800 in.-kips, and that corresponding to shear capacity is about 1650 in.-kips. The corresponding lateral capacities are 104 kips (flexure) and 100 kips (shear). The strengthened specimens could therefore be expected to fail by combined shear and flexure.

2.7 Strengthened Specimen 1-3

2.7.1 Details. The strengthening technique used for Specimen 1-3, shown in Fig. 2.8, consisted of the same basic reinforced shotcrete jacket, plus #6 longitudinal bars at each midface. Holes were drilled through the column, and #3 crossties, secured with epoxy, anchored opposite face longitudinal bars. Holes were 1/4 in. oversize and were cleaned using a tight-fitting bottle brush. One end of each crosstie was field-bent around the midface bar before the epoxy had set.

2.7.2 Calculated Strengths. Neglecting the contribution of the crossties, theoretical moment and shear capacities are identical to those of Specimen 1-2 (Fig. 2.7) [15].

2.8 Repair of Specimen 1-1

Following the first test, Specimen 1-1 was removed from the test frame for repair and strengthening. After removing all loose cover (Figs. 2.9, 2.10), jacket reinforcement (Fig. 2.8) was constructed identical to that used for Specimen 1-3, as shown in Fig. 2.11. Crossties through the cracked column core were secured by epoxy (Fig. 2.12), and a shotcrete jacket was added to increase the column size to 17 by 17 in.

2.9 Fabrication of Strengthened Specimens

Fabrication of strengthened specimens consisted of tieing the jacket reinforcement cages and then shotcreting. Specimens were roughened by light sandblasting using a No. 6 venturi nozzle and a fine sand (No. 6). As shown in Fig. 2.13, wooden screed guides were attached to each specimen's end blocks using ramset nails. Shotcrete quality was monitored using two vertical test panels (36 x 18 x 3 in.), shown in Fig. 2.14. One of the panels had a wood back while the other had a concrete back. The two types of materials were used to determine if shotcrete test panel rebound characteristics different from the actual column applications might alter quality control information. Half of each panel was reinforced identically to the jacket of Specimen 1-3, without crossties. Two sizes of core samples were to be taken from each panel. Large cores (4 x 3 in.) from the reinforced side of each panel were used to monitor void formation behind individual bars. Small cores (1-3/4 x 3 in.) from the

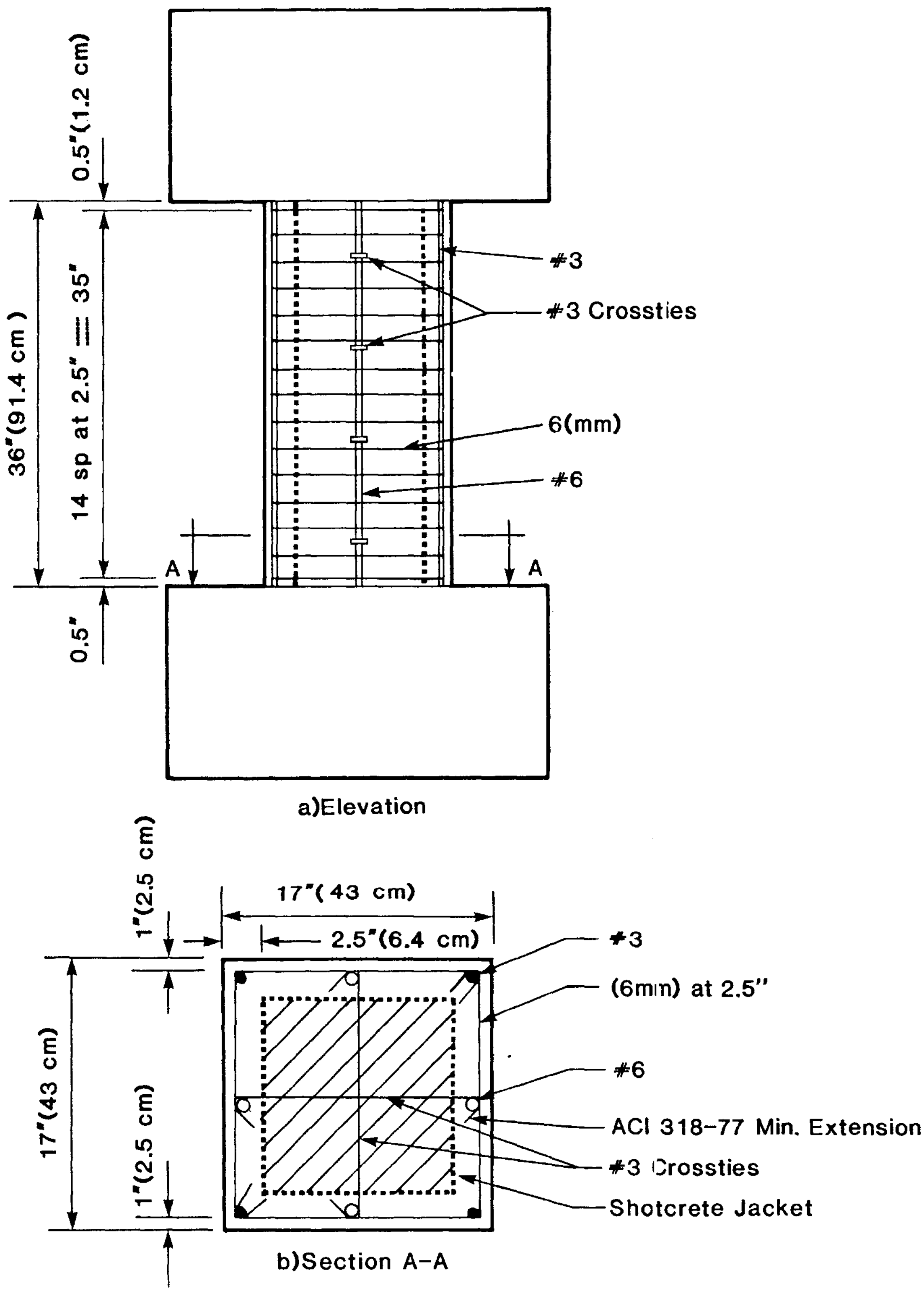

Fig. 2.8 Details of Specimen 1-3.

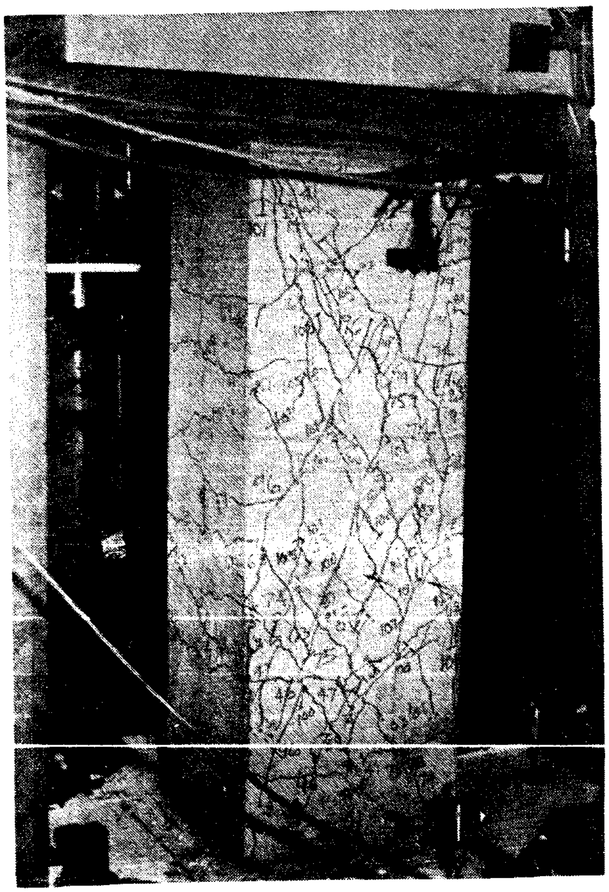

Fig. 2.9 Post-test, Specimen 1-1

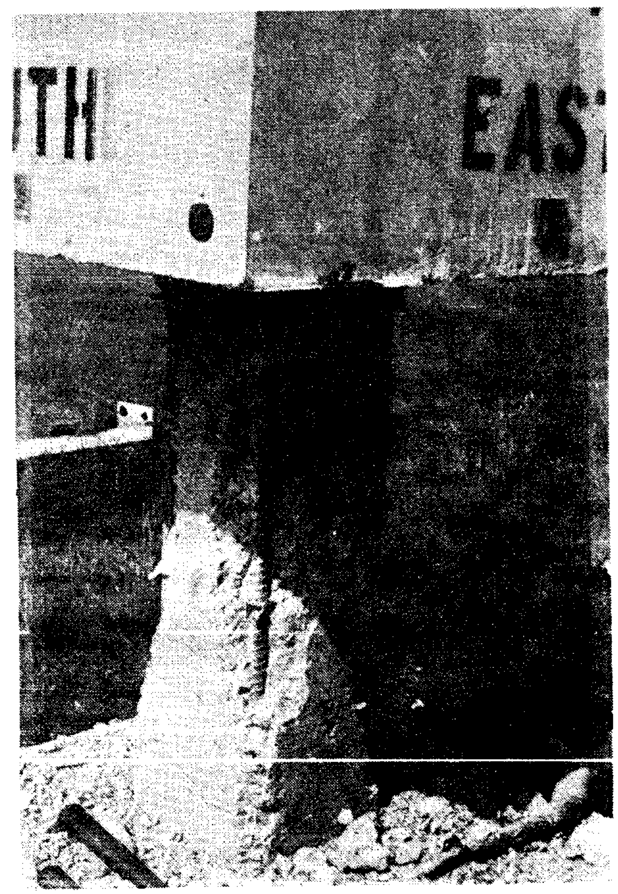

Fig. 2.10 Loose cover removed, Specimen 1-1

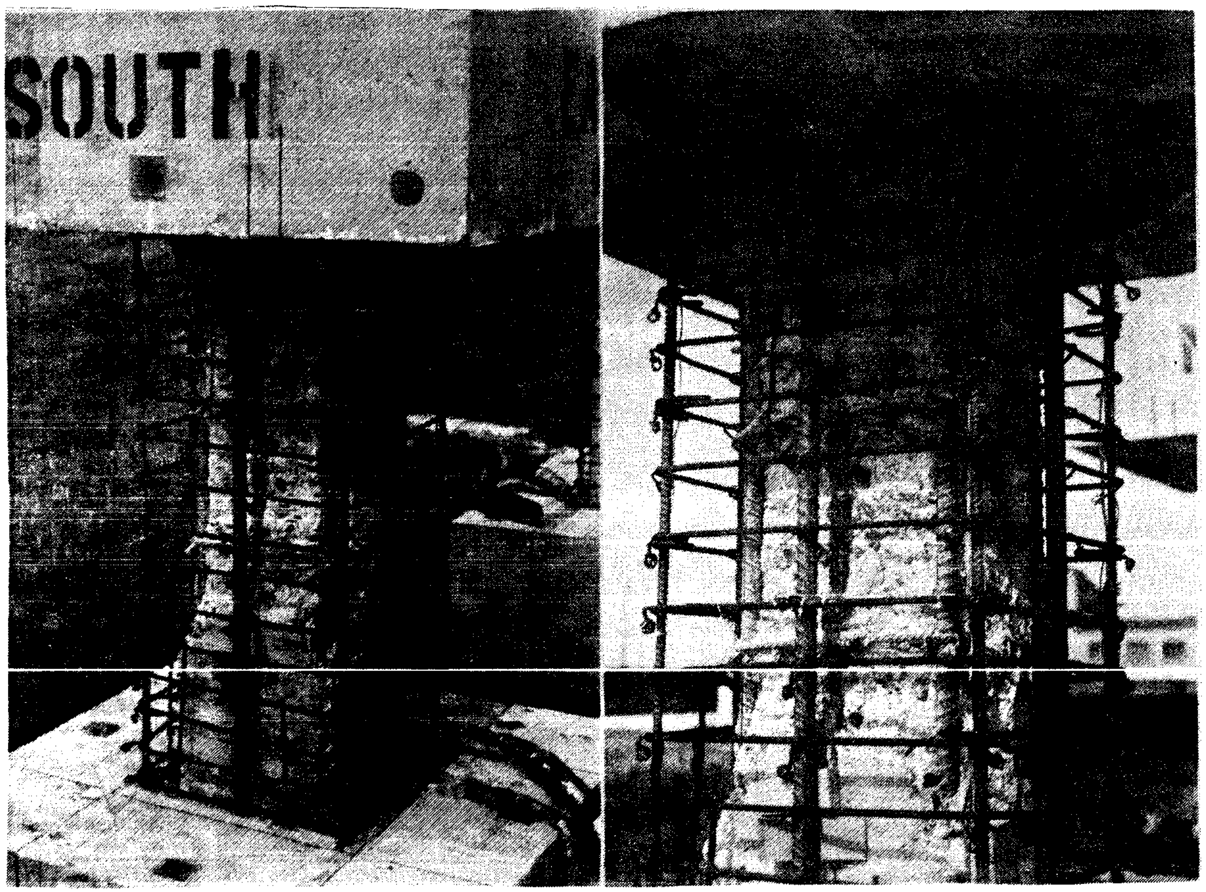

Fig. 2.11 Jacket reinforcement, Specimen 1-1

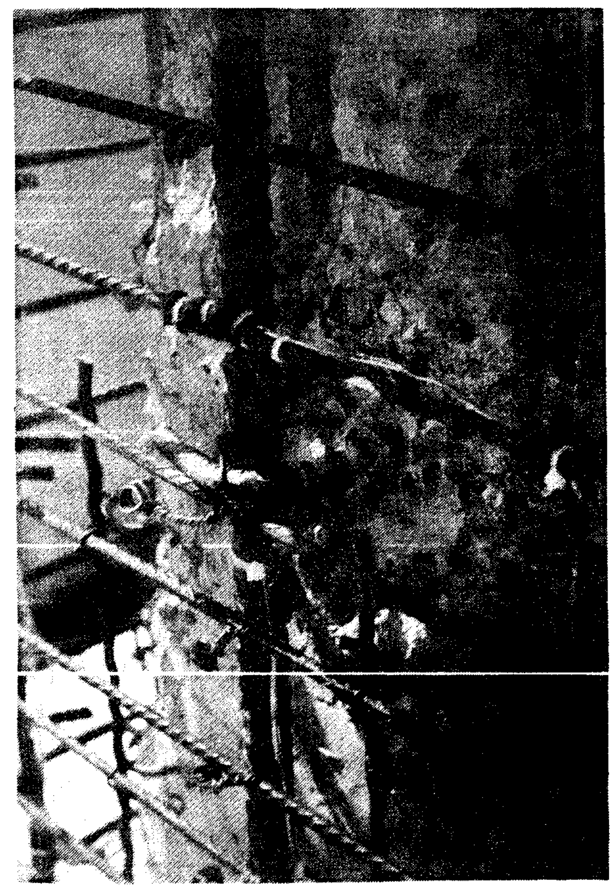

Fig. 2.12 Crossties secured by epoxy, Specimen 1-1

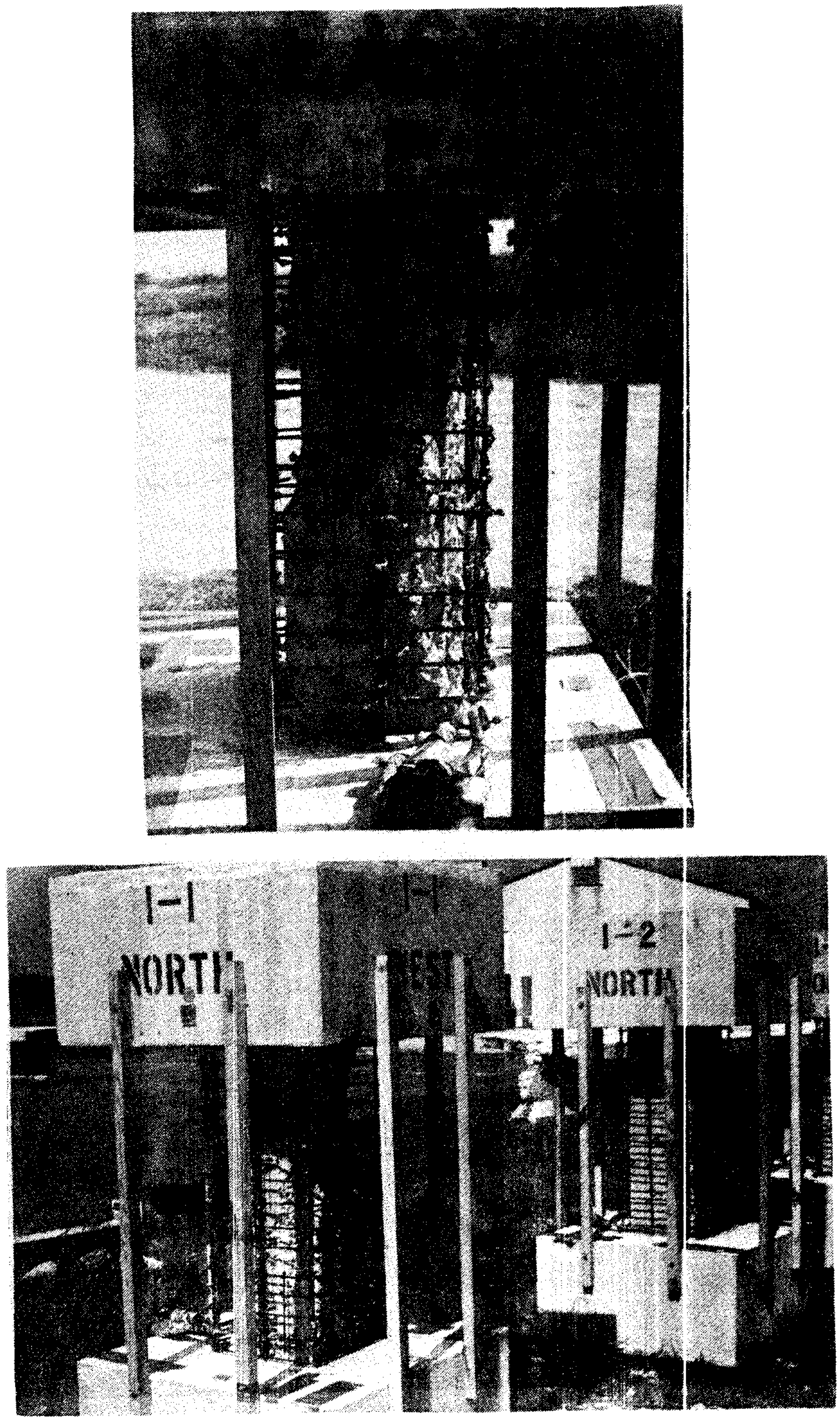

Fig. 2.13 Screed guides

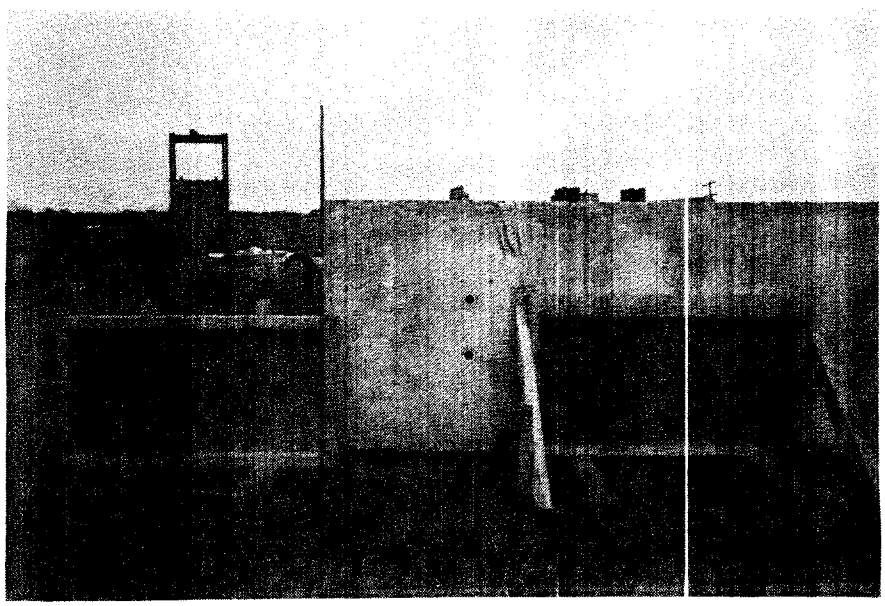

Fig. 2.14 Shotcrete test panels

unreinforced side were used for compressive strength tests. An experienced contractor shotcreted and float-finished (Figs. 2.15, 2.16) the specimens and panels, both of which were cured under polyethylene sheets for seven days. When the specimens were shotcreted, concrete temperature, slump, unit weight, and air content were measured. Two sets of control cylinders were cast; one set was taken using concrete directly from the ready-mix truck, the other set was taken using shotcrete placed in a wheelbarrow by the nozzle.

2.10 Material Characteristics of Strengthened Specimens

2.10.1 Shotcrete. Ready-mixed concrete was obtained from a local supplier for the shotcrete. Mix proportions for the shotcrete [18] were as shown in Table 2.4.

TABLE 2.4 Shotcrete

Shotcrete Properties	
Slump (in.) (from truck)	5-1/2
Unit Weight (lbs/ft^3) (from truck)	130
Air Content (%) (from truck)	4-1/2
Air Content (%) (from nozzle)	4
Shotcrete Mix Design (4000 psi) Proportions for 1 yd^3	
Water	250 lb
Cement	658 lb
Fine Aggregate	2100 lb
Coarse Aggregate (3/8 in.)	750 lb
Sol Air (3% air entrainment)	10 oz
CCC 494 (water reducing agent) (w/c = 0.38 by weight)	21 oz

The aggregate was Colorado River sand and gravel. To facilitate pumping, a small quantity of pumping agent [20] was added on site. Table 2.4 summarizes the shotcrete properties.

Four-inch cores (Figs. 2.17, 2.18) were taken from both the concrete-backed panel (CB) and the wood-backed panel (WB) to determine if voids were present behind the reinforcing. A single small void (1/4 x 1/4 in.) was found in one (CB) of the six samples. There was virtually no difference between the wood or concrete-backed panel

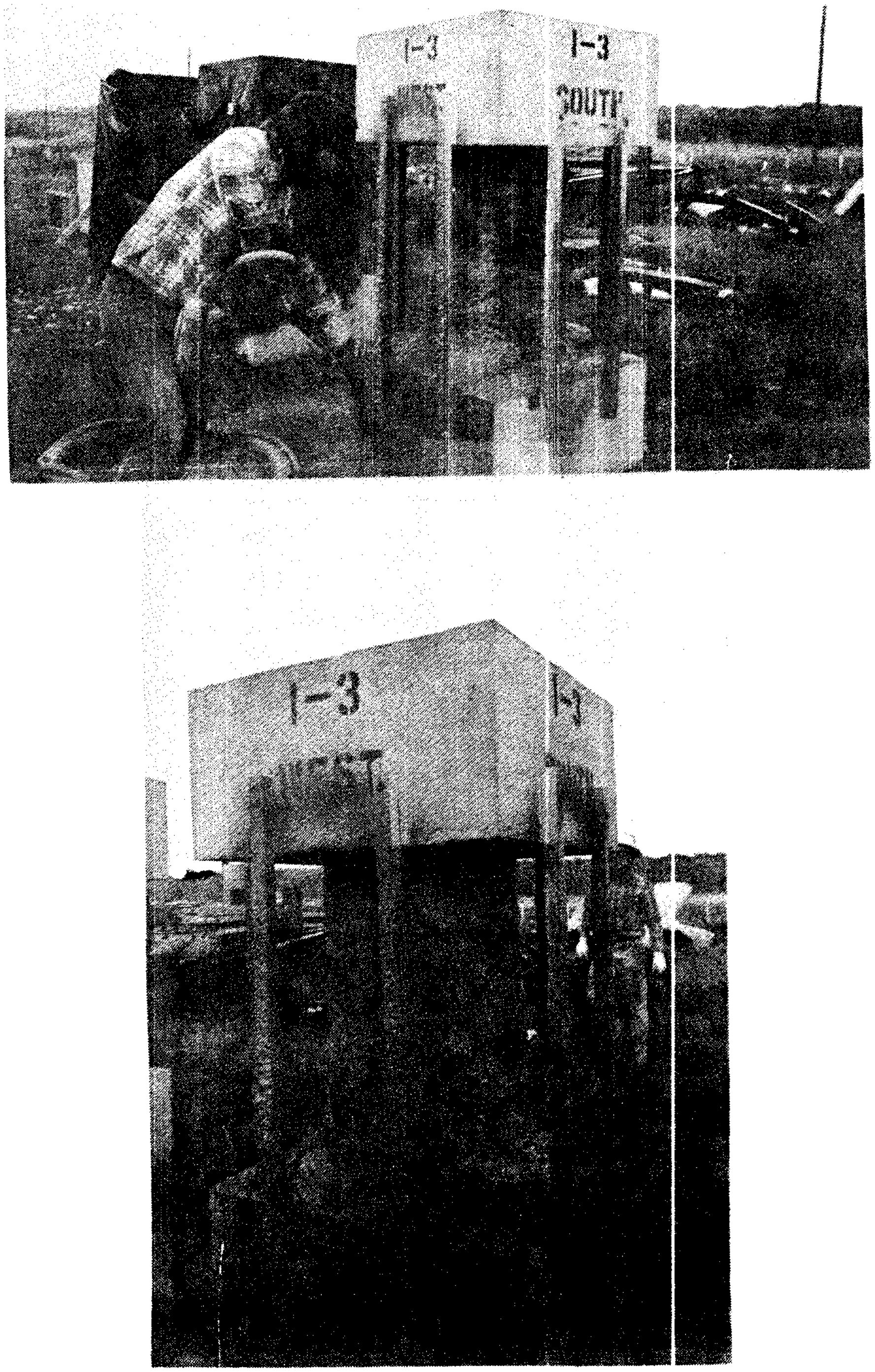

Fig. 2.15 Shotcreting

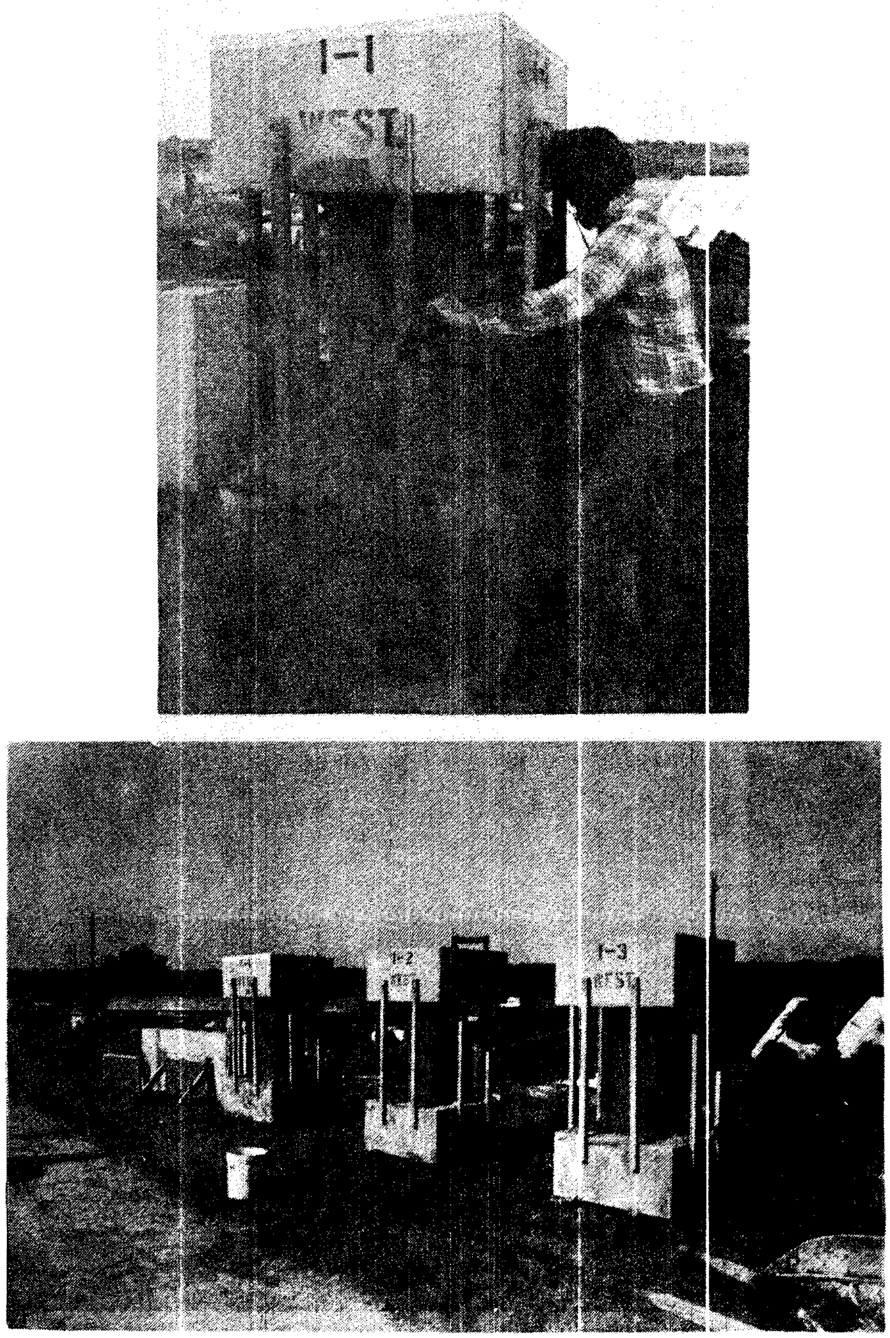

Fig. 2.16 Finishing shotcrete

Fig. 2.17 Panel (top) core samples

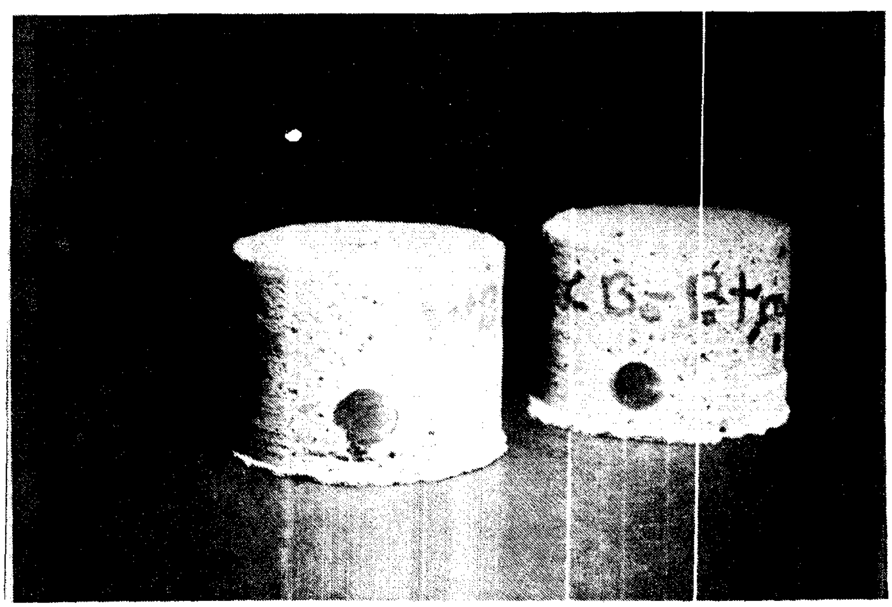

Fig. 2.18 Panel (bottom) core samples

samples Smaller cores (1-3/4 x 3 in.) were taken from both panels, capped and tested in compression, with the results shown in Table 2.5.

2.10.2 Reinforcement. Jacket reinforcement consisted of #6 longitudinal bars at column midfaces, #3 crossties and longitudinal bars at corners, and 6 mm deformed ties. All U.S. sizes conformed to ASTM A-615, Gr. 60. Data on the #6 and 6 mm bars were provided in Section 2.4.2. Samples of the #3 bars were tested to obtain the averaged steel properties shown in Table 2.6, and the typical stress-strain curve of Fig. 2.19.

2.10.3 Epoxy. Crossties (#3's) were anchored to the original column using Concresive 1411, a two-component paste epoxy bonding agent produced by Adhesive Engineering [19]. Minimum mechanical properties are summarized in Table 2.7.

2.11 Loading History

Axial compression was maintained at 64.8 kips for all tests, and was based on typical column load data [14]. The corresponding compressive stress was 450 psi for the 12- x 12-in. column (Test 1), and 224 psi for the 17- x 17 in. columns (Tests 2, 3, and 4).

The lateral loading history (Fig. 2.20) was displacement controlled. Specimen 1-1 was limited to 2% drift, while Specimens 1-2, 1-3, and 1-1R had maximum drifts of 2.5%. Each test consisted of two cycles at low load levels for system checkout, followed by sets of three cycles at increasing displacement levels. Drift was increased in increments of 0.5%.

TABLE 2.5 Shotcrete Strengths

	Age (days)	f'_c (psi)	Average f'_c (psi)
From ready-mix truck	28	4562	4692
	28	4704	
	28	4810	
From nozzle	28	5093	5152
	28	5270	
	28	5093	
Concrete-backed panel	107	3651	3037
	107	3143	
	107	2295	
	107	3343	
	107	2753	
Wood-backed panel	107	4058	2905
	107	2528	
	107	3193	
	107	2844	
	107	1904	

TABLE 2.6 Steel Properties (Jacket #3 Long)

Bar Size	f_y (ksi)	E (ksi)		E_{sth} (ksi)	f_u (ksi)	
#3	75	26923	0.010	1182	114	0.117

TABLE 2.7 Concresive 1411 Mechanical Properties

Tensile Strength (psi)	1500
Elongation at Break (%) (ASTM 0638)	. 4
Compressive Yield Strength (psi)	8000
Compressive Modulus (psi) (ASTM D695)	4.0×10^5
Heat Deflection Temperature (°F) (ASTM D648)	105
Slant Shear Strength (psi)	75000
Damp to Damp Concrete (AASHTO T-237)	100% concrete failure

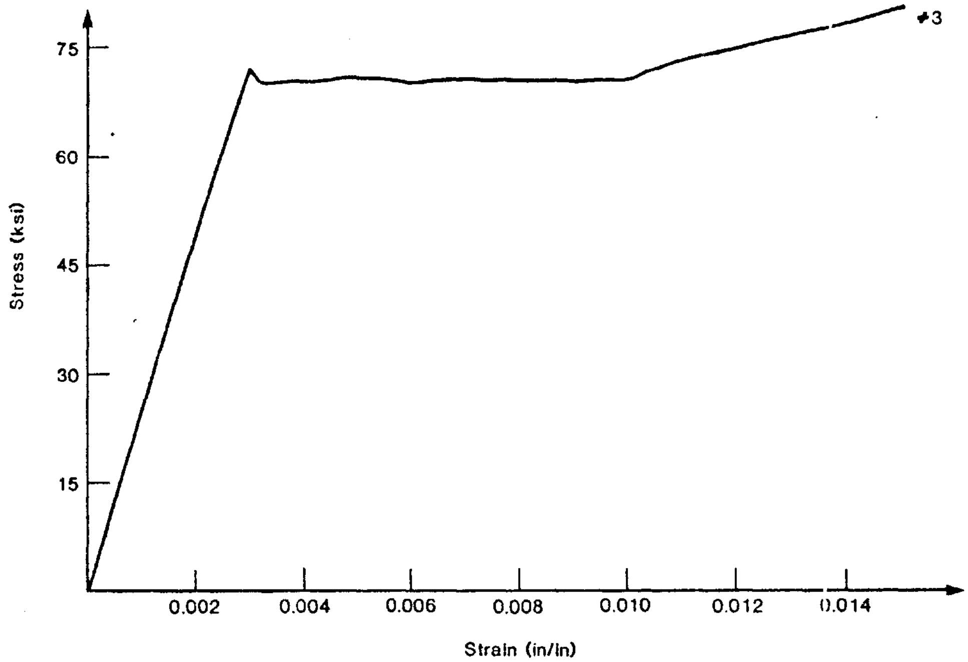

Fig. 2.19 Stress-strain curve for jacket steel (#3)

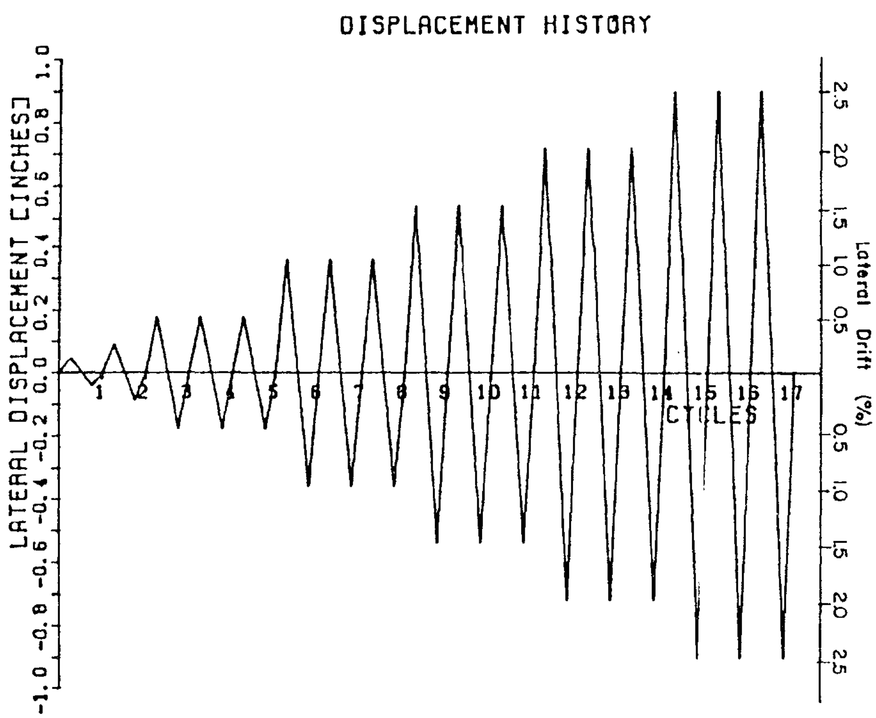

Fig. 2.20 Lateral displacement history

CHAPTER 3

LOADING SYSTEM AND INSTRUMENTATION

3.1 Loading System

In this research program, the specimens were loaded laterally in one direction while a constant axial load was maintained. The loading system utilized the reinforced concrete floor-wall reaction system [5] in Ferguson Laboratory.

The loading system consists of three independent components: 1) a mechanically-controlled hydraulic system for controlling the axial load; 2) a closed-loop, servo-controlled hydraulic system for controlling the lateral load; and 3) cross-coupled hydraulic rams for restraining the end blocks from rotating during loading.

The axial loading system was made up of a 300-kip static capacity ram connecting the specimen's upper loading head with the vertical reaction frame. Axial loads were adjusted manually using an Edison load maintainer [21] while monitoring load cell readings. The lateral loading system was composed of two rams, an accumulator, servo-controller, and a central pump. Each ram had a tensile static capacity of 113 kips with a piston stroke of 12 in. The lateral rams were under displacement control. Figure 3.1 illustrates the arrangement of the loading rams with respect to the specimen, and Fig. 3.2 illustrates the actual test setup.

The test specimen is bounded at each end by a loading head which is a welded assembly of wide flange members. The end blocks of the specimen were attached to the loading heads by eight high-strength threaded rods, after placing a coat of gypsum plaster between the loading head and the end block to ensure a smooth bearing surface. The lower loading head is bolted to the testing floor, while the upper crosshead is free to translate in the north-south direction.

The test specimen represents a column bounded by very stiff framing elements. To better model the condition of end fixity, rotations of the upper loading head are restrained by a system of cross-coupled hydraulic rams (Figs. 3.3, 3.4). Two pairs of rams act vertically to restrain rotations of the upper head in two orthogonal vertical planes. The remaining pair of rams is used to resist rotation of the upper head about a vertical axis.

Each pair of cross-coupled rams may extend or retract equally, as in the case of vertical translation of the upper loading head. However, because of cross-coupling, one ram in a pair cannot

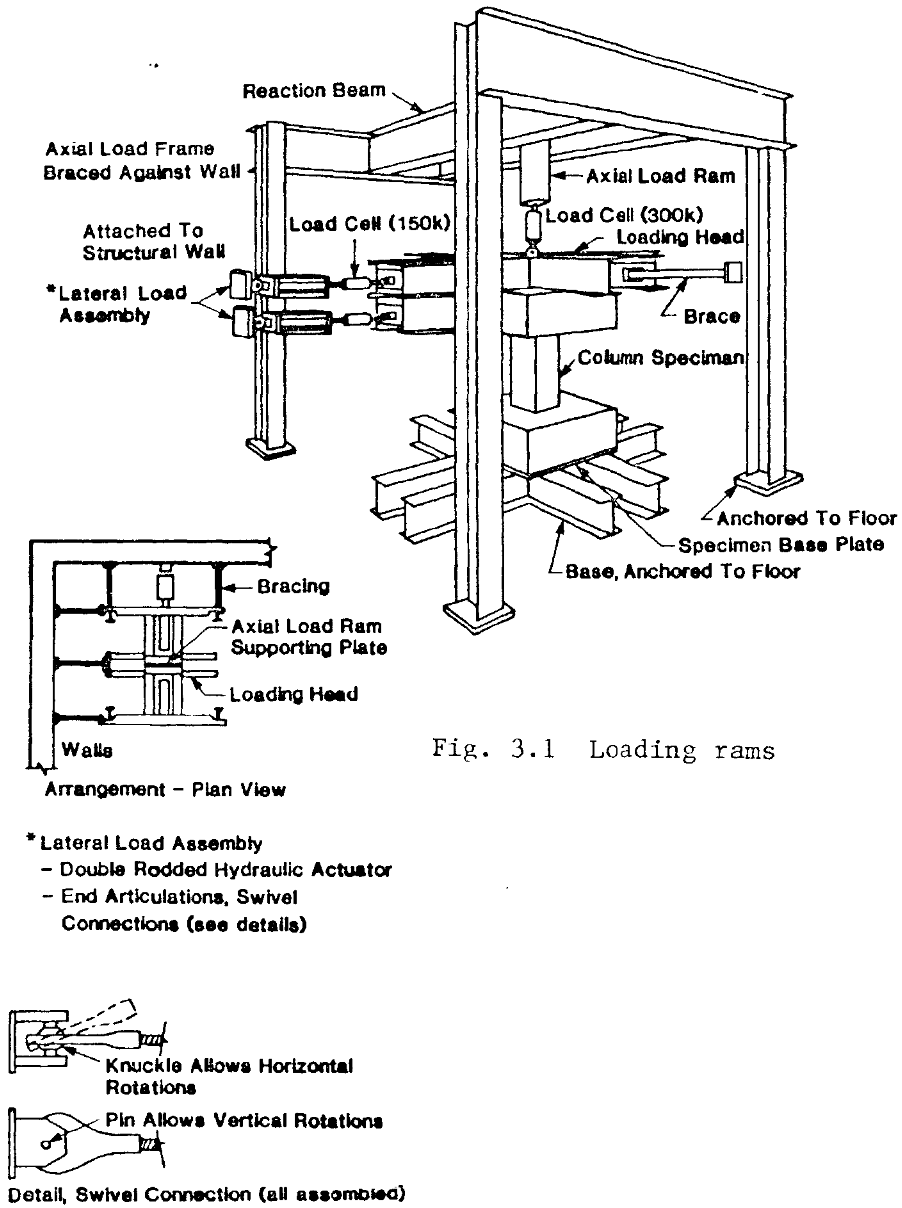

Fig. 3.1 Loading rams

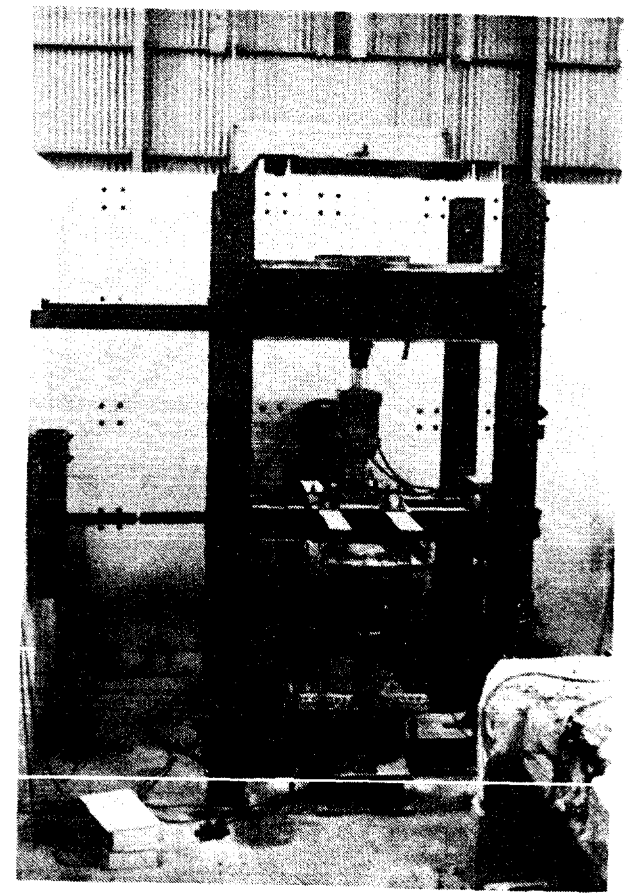

Fig. 3.2 Test setup

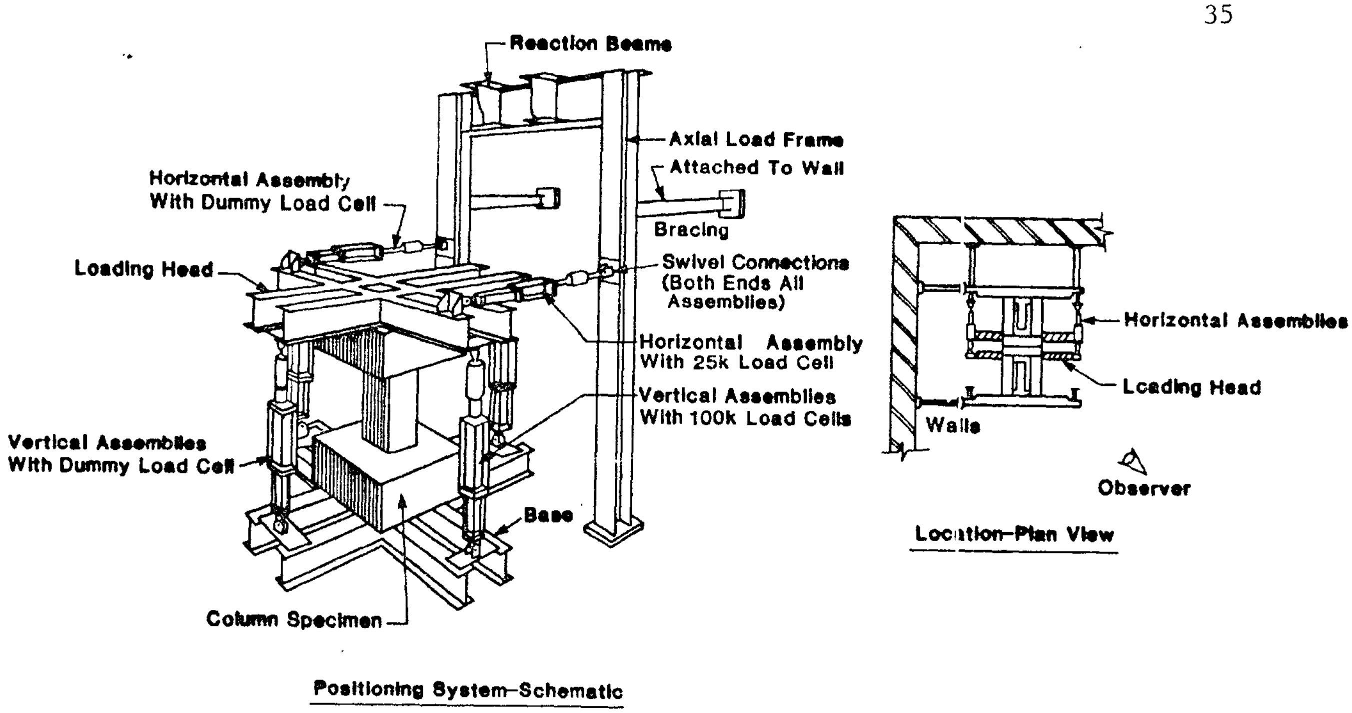

Fig. 3.3 Restraining rams

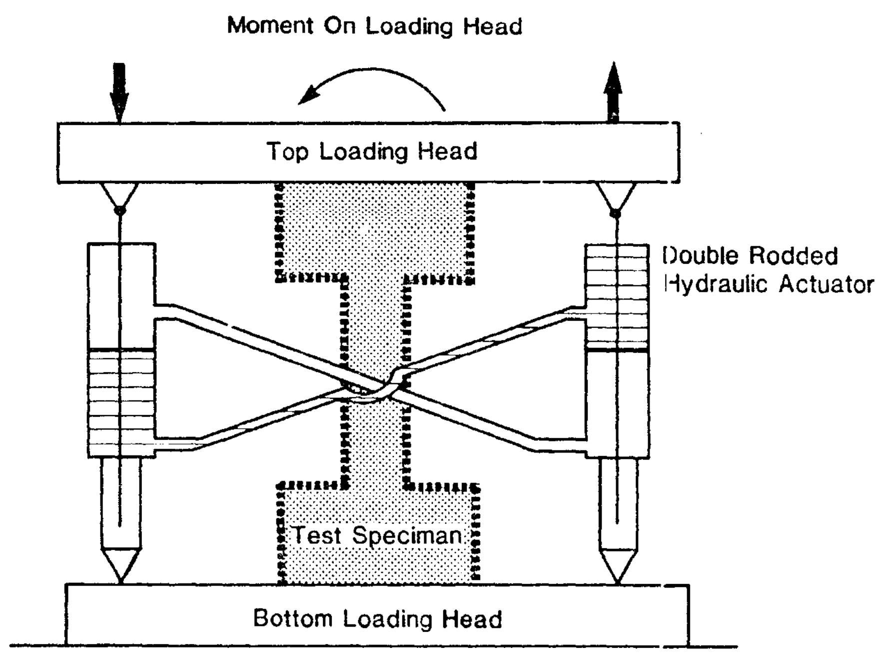

Vertical and Horizontal Positioning System

Fig. 3.4 Vertical and horizontal positioning system retract while the other ram extends. This resistance to differential displacements restrains rotation of the upper loading head.

3.2 Instrumentation

Three types of measuring devices were used to monitor the performance of the specimen during testing: 1) load cells; 2) linear potentiometers; and 3) strain gages.

3.2.1 Loads. Load cells were mounted on each loading ram and on one ram in each pair of restraining rams. All load cells were monitored by the data acquisition system, and the force applied by one of the lateral loading rams was plotted on an X-Y recorder as the test progressed.

3.2.2 Deflections. Twelve linear potentiometers were used to monitor the deflections and rotations of the specimen end blocks. The potentiometers were supported independently of the loading frame. Deflections measured by the potentiometers were recorded by the data acquisition system. The signal from one of the lateral potentiometers, when used in conjunction with the output from a lateral ram load cell, provided a load-deflection plot along the north-south displacement axis used to monitor the response during testing.

3.2.3 Strains. As shown in Figs. 3.5 and 3.6, paper backed strain gages were attached to the tie and longitudinal reinforcement in both the column core and shotcrete jacket. Gages were located on each leg of a jacket reinforcement tie at three levels (top, mid-height, and bottom) of the column. One end of every crosstie was gaged.

3.2.4 Slip. Relative slip between the original column and the jacket was measured using slip wires as shown in Fig. 3.7 located at the column mid-height and near the base.

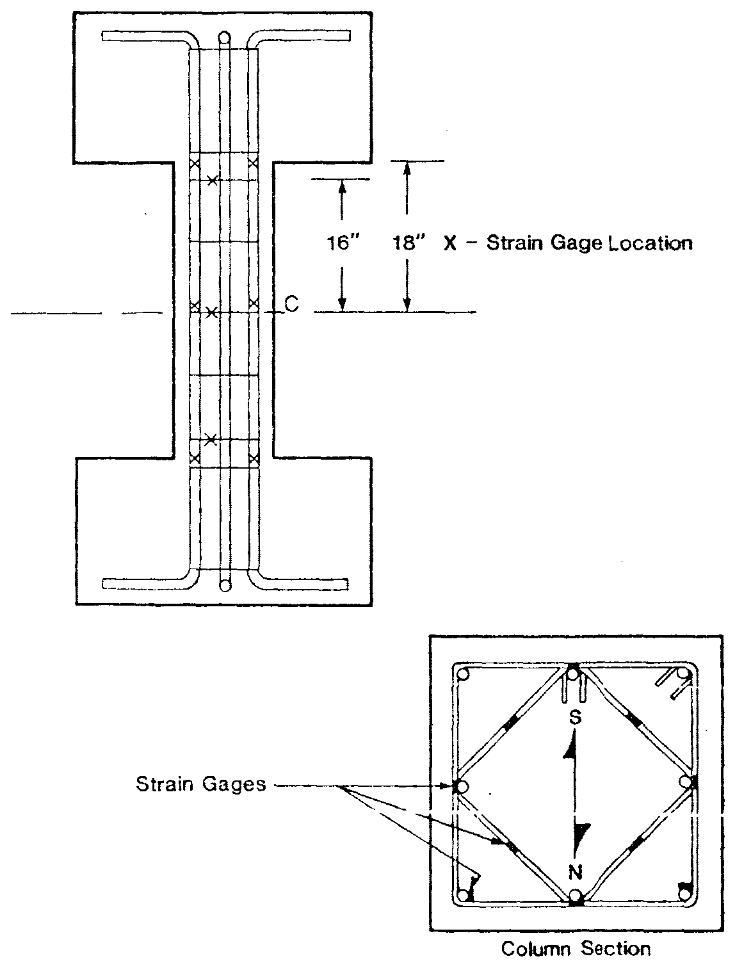

Fig. 3.5 Strain gage locations (original specimen)

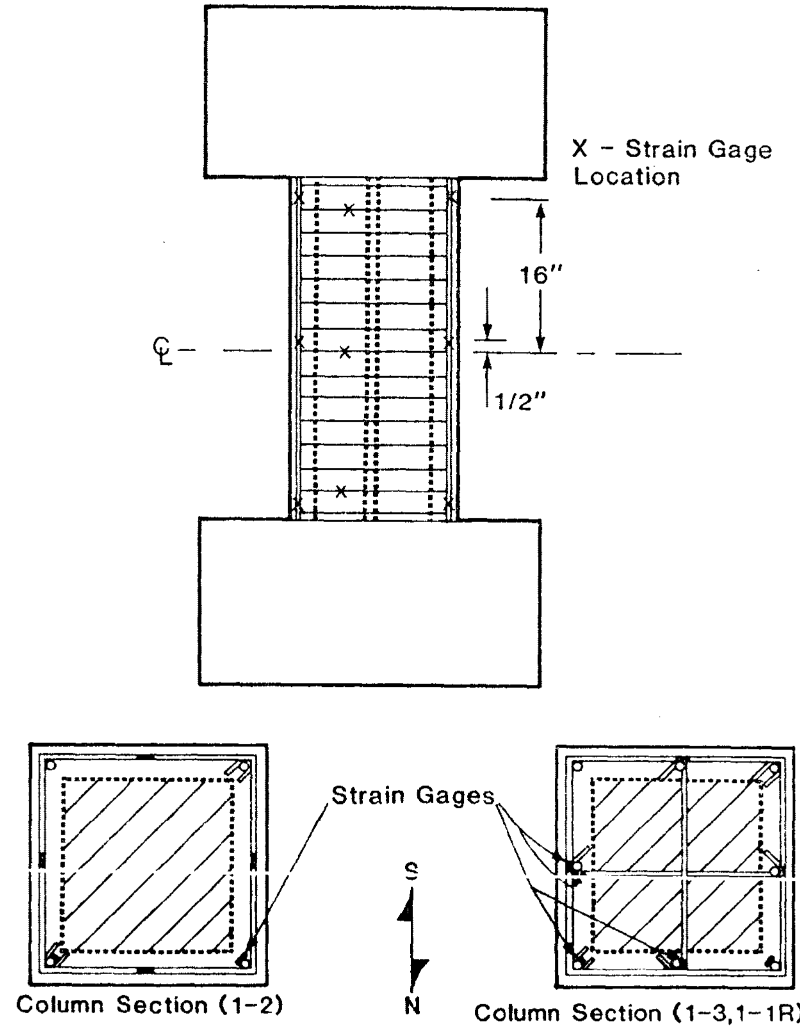

Fig. 3.6 Strain gage locations (jacket)

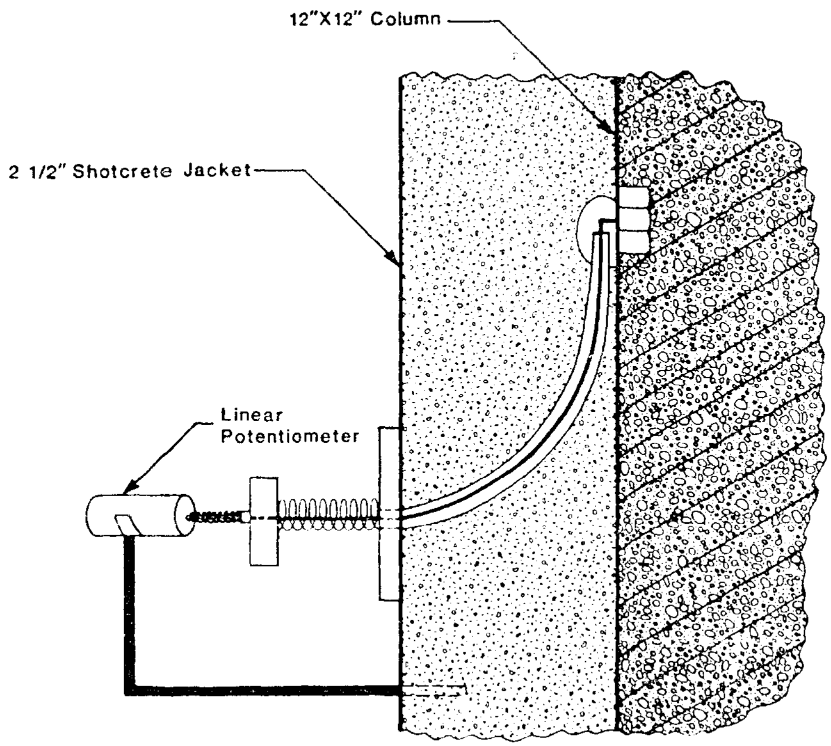

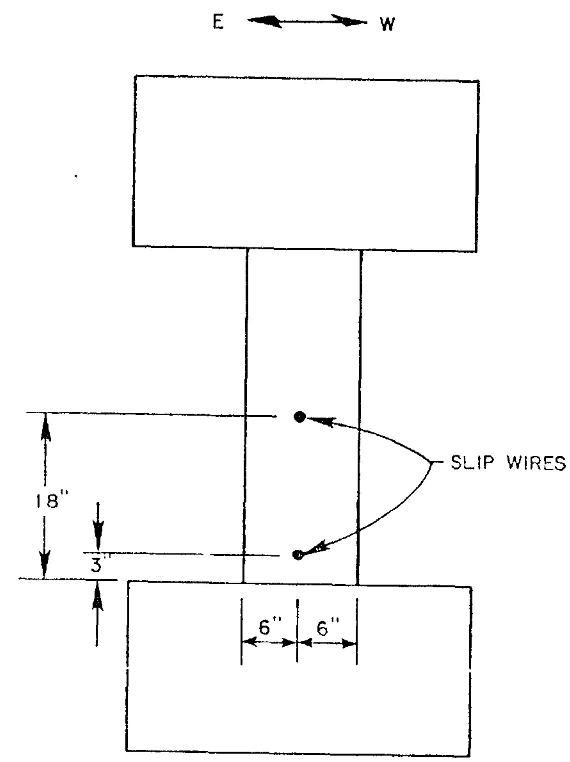

Fig. 3.7 Slip wire instrumentation

CHAPTER 4

BEHAVIOR OF SPECIMENS

4.1 Introduction

Portions of the experimental test results for all specimens (original, strengthened and repaired) are reported in this chapter. Load-deflection curves and envelopes for all specimens are shown. Strain information is reported for Specimen 1-1 and Specimen 1-3 only because strain data from Specimen 1-3 were found to be representative of both the other strengthened specimen (1-2) and the repaired specimen (1-1R). Significant variations among individual tests will be discussed in Chapter 5. Basic data for each test were obtained from load cells, displacement transducers and strain gages. Photographs were used to record crack patterns at the end of each load phase.

The hysteretic behavior of the test specimens under the imposed cyclic deformations and constant axial load is presented in terms of lateral load-deflection curves. Of particular interest are the stiffness of the specimen, its peak lateral capacity at a given deflection level, its loss of lateral load capacity due to cycling, and the overall shape of the hysteretic loops. The slope of the load deflection curve at any point represents the tangent stiffness of the specimen. Envelopes of peak lateral load-deflection values are used for direct comparison of test results. The main objective in analyzing the test results is to study the differences in behavior between the original column, and the same type of column after strengthening or repair.

4.2 Description of Test Results

4.2.1 Load-Deflection Curves. Load-deflection curves for Specimens 1-1, 1-2, 1-3, and 1-1R are shown in Figs. 4.1 through 4.4. Inspection of the figures reveals recognizable characteristics such as symmetry about the load axis, peak load-displacement envelope outlines and the effect of successive cycles at a constant drift level. Hysteretic behavior is referred to as "stable" when only small changes in lateral capacity are observed under cycling to constant drift levels. Large losses in specimen stiffness are characterized by "pinching" of the hysteretic loops. Poor energy dissipating characteristics of a member are generally typified by nonstable hysteretic behavior with pinching. As expected, pinching is more pronounced for both the original column (Specimen 1-1) and the repaired column (Specimen 1-1R), than for either of the strengthened specimens (Specimens 1-2, 1-3). Peak load-deflection envelopes, shown in Fig. 4.5, connect peak load-deflection values in the first cycle to each drift level, and are used to compare hysteretic characteristics

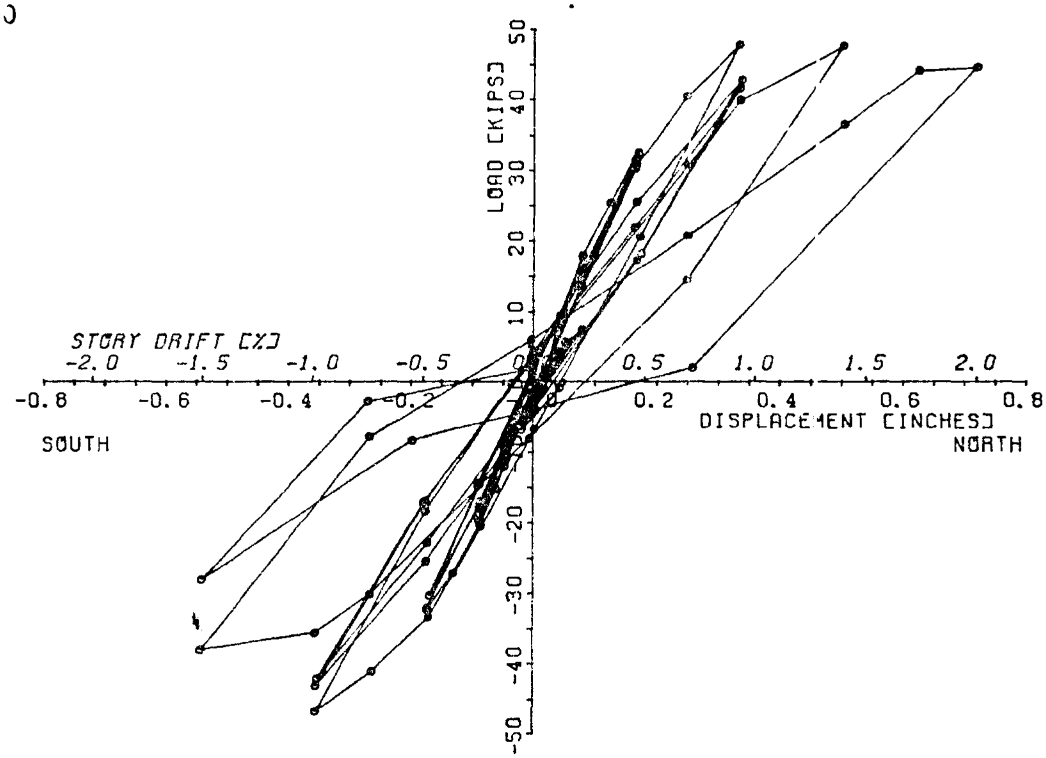

Fig. 4.1 Load-deflection curve, Specimen 1-1

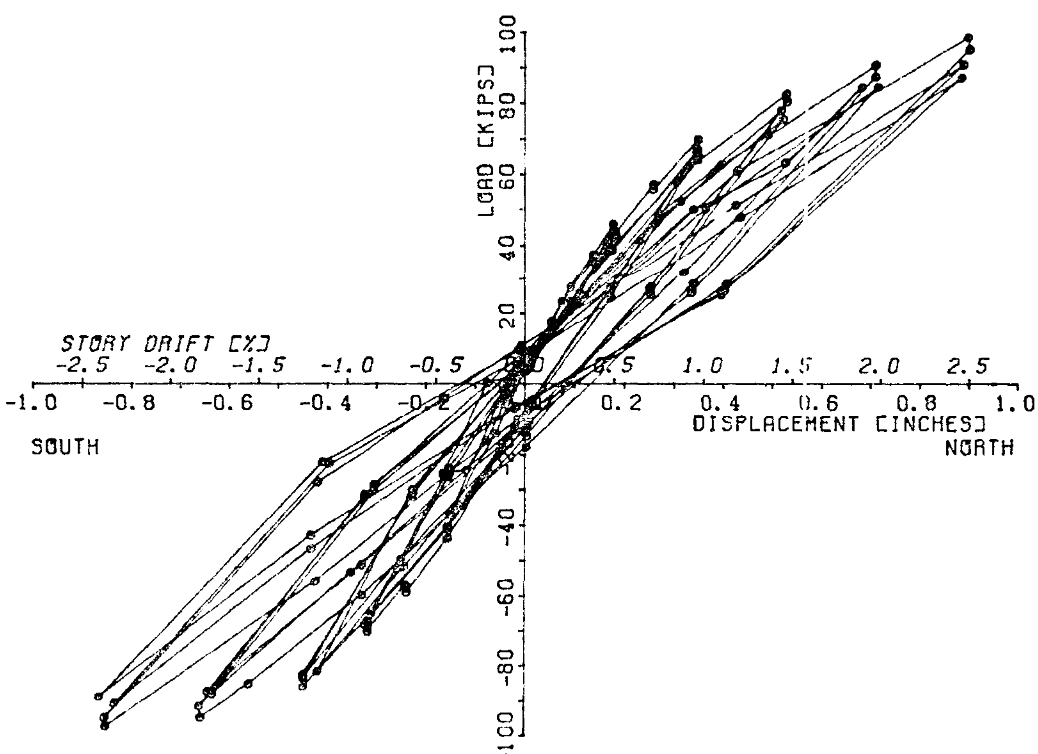

Fig. 4.2 Load-deflection curve, Specimen 1-2

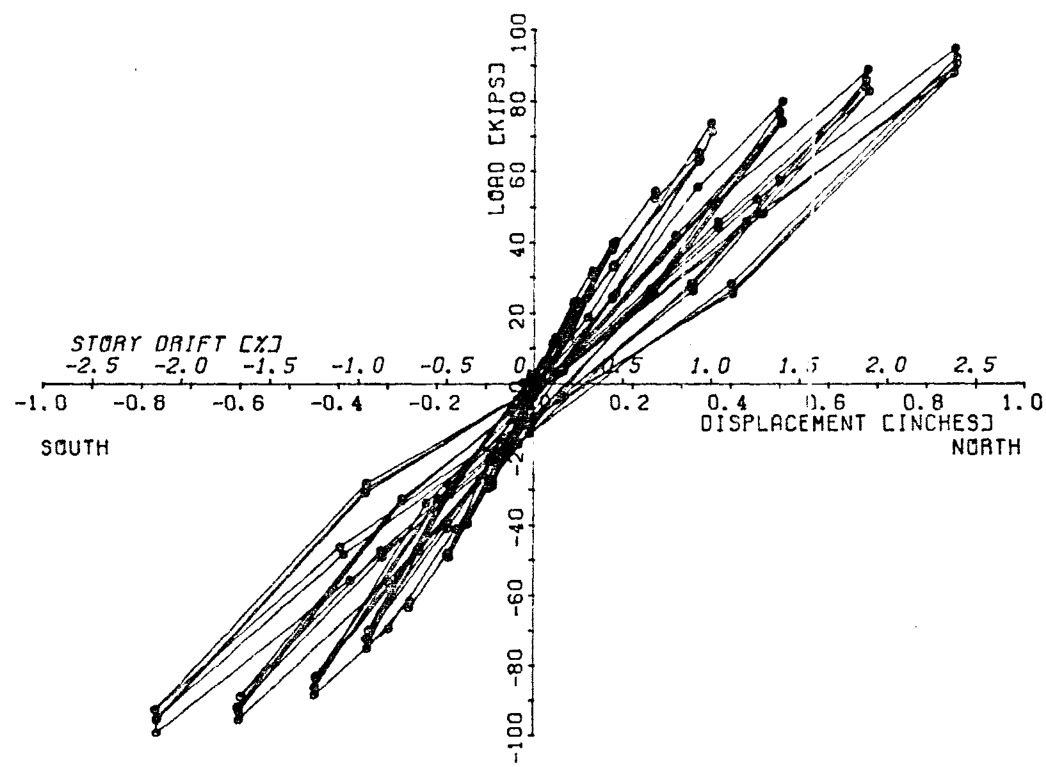

Fig. 4.3 Load-deflection curve, Specimen 1-3

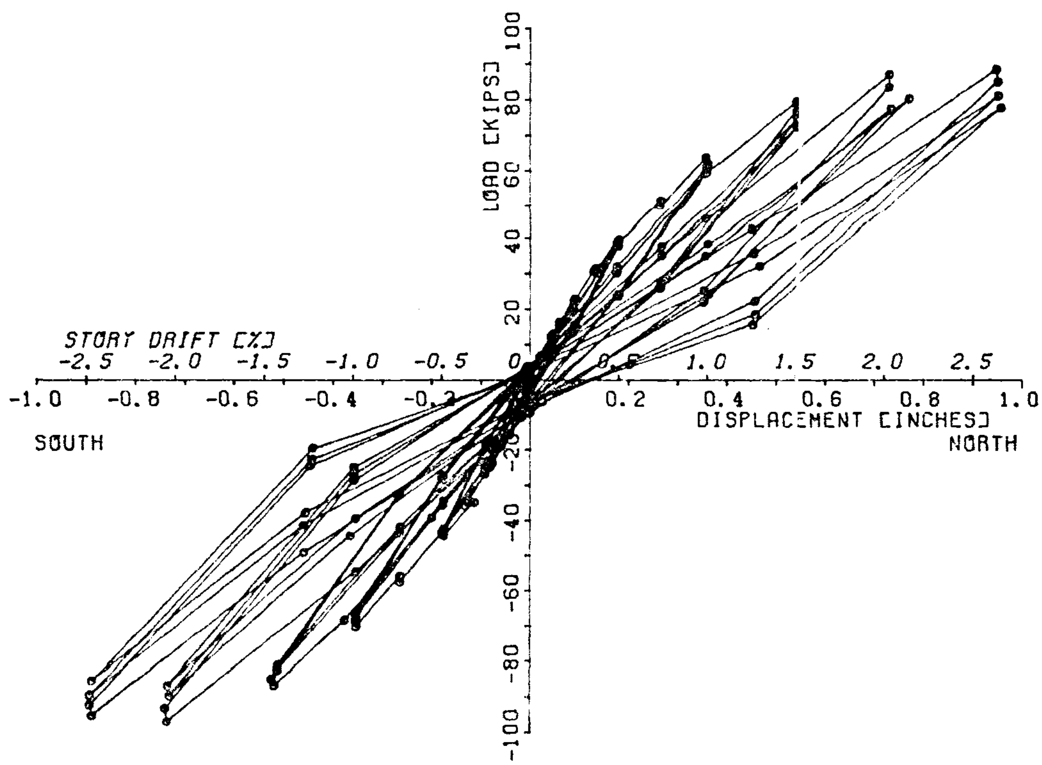

Fig. 4.4 Load-deflection curve, Specimen 1-1R

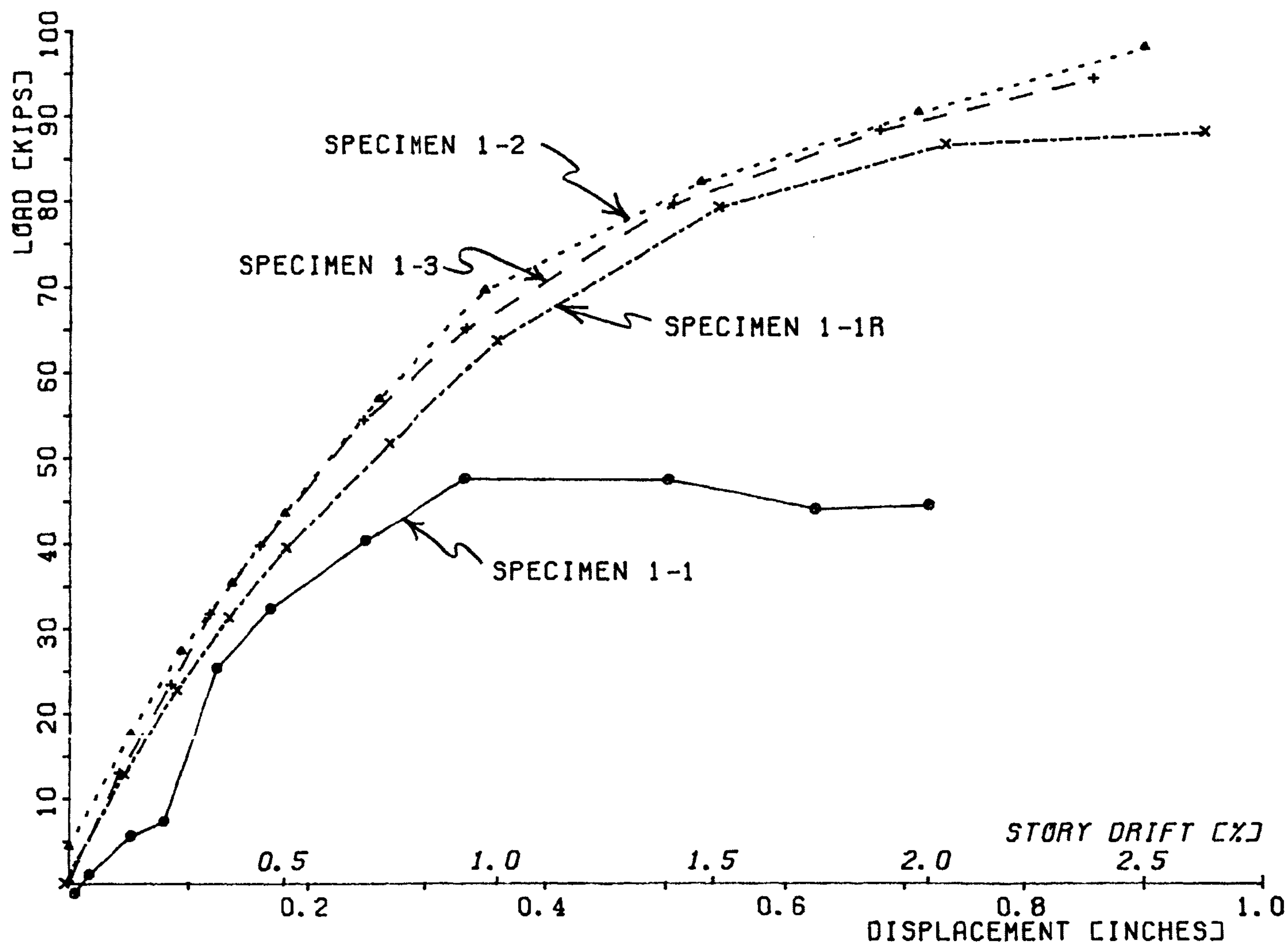

Fig. 4.5 Load-deflection envelopes, Specimens 1-1, 1-2, 1-3, and 1-1R

of different tests. North and south displacements generated similar peak load envelopes, and for clarity of presentation only the north displacement curves are shown. For lateral deflections in excess of 1 percent drift, the lateral load capacity of Specimer 1-1 is observed to decay much faster than that of either of the strengthened specimens. The repaired specimen (1-1R) was less stiff than either of the two strengthened specimens, and exhibited significantly reduced lateral capacity at deflections in excess of 2% drift.

4.2.2 Crack Patterns. Crack patterns for each of the tests were photographed at the end of each load phase, Figs. 4.6 through 4.9. Figure 4.6 illustrates typical crack patterns on the northwest faces of Specimen 1-1 after reaching lateral displacements corresponding to 0.5, 1, 1.5, and 2% drift. At 0.5% drift, flexural cracks developed near the top and bottom face of the column. Inclined shear cracks formed at 1% drift, and were approximately 1/64 in. wide at that displacement level. Cycling at 1.5% drift extended those inclined cracks across the column face to a width of 1/32 in. When 2% drift was reached, the inclined cracks widened, and concrete spalling was observed at the column corners, and to a lesser degree on the column face at mid-height.

Typical crack patterns for the west face of Specimen 1-3 are shown in Fig. 4.8, for lateral drifts for 1.0%, 1.5, 2, and 2.5%. Significant flexural cracks developed at the 1% drift level and were less than 1/64 in. wide. Inclined cracks developed from existing flexural cracks at 1.5% drift, and a wide crack (3/32 in.) on the opposite side of the displacement direction opened up between the shotcrete jacket and the top and bottom end blocks. Continued cycling at 2% drift level extended and widened both inclined and end cracks, culminating in crushing and spalling near both top and bottom end blocks at the 2.5% drift level. At peak displacements at that drift level, the end cracks were approximately 1/4 in. wide.

Similar crack patterns were observed in Specimens 1-1 and 1-1R for all levels of deformation. Flexural cracks turned into inclined cracks at about 1% drift. Repeated cycling at 1% drift widened and extended those cracks, which were evenly distributed over the height of the column. The cracking patterns of Specimens 1-2 and 1-3 resemble each other, but were significantly different from those of Specimens 1-1 and 1-1R. The strengthened specimens showed only flexural cracking at 1% drift. Cracks became inclined at 1.5% drift. At corresponding drift levels, Specimens 1-2 and 1-3 had fewer cracks and a smaller relative crack width than Specimens 1-1 and 1-1R. Specimen 1-1 exhibited some spalling at column mid-height, while Specimens 1-2, 1-3 and 1-1R all exhibited nearly equal amounts of crushing near the end blocks. Summarizing, Specimens 1-1 and 1-1R exhibited shear-dominated crack patterns, and Specimens 1-2 and 1-3 exhibited flexure or flexure-shear dominated crack patterns.

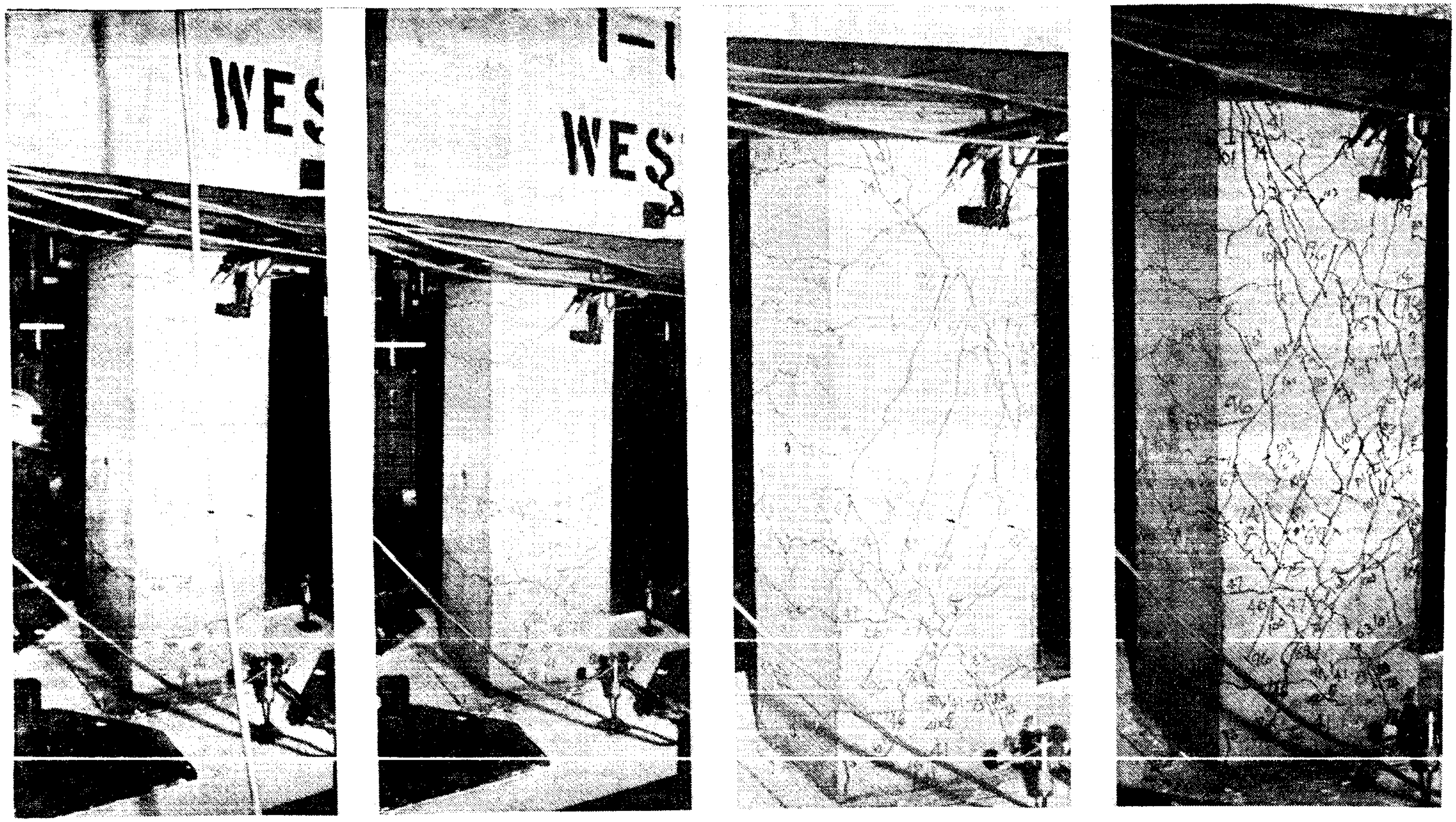

(a) 0.5% drift (b) 1.0% drift (c) 1.5% drift (d) 2.0% drift

Fig. 4.6 Crack patterns, NW column faces, Specimen 1-1

(a) 1.0% drift　(b) 1.5% drift　(c) 2.0% drift　(d) 2.5% drift

Fig. 4.7 Crack patterns, Specimen 1-2

(a) 1.0% drift (b) 1.5% drift (c) 2.0% drift (d) 2.5% drift

Fig. 4.8 Crack patterns, Specimen 1-3

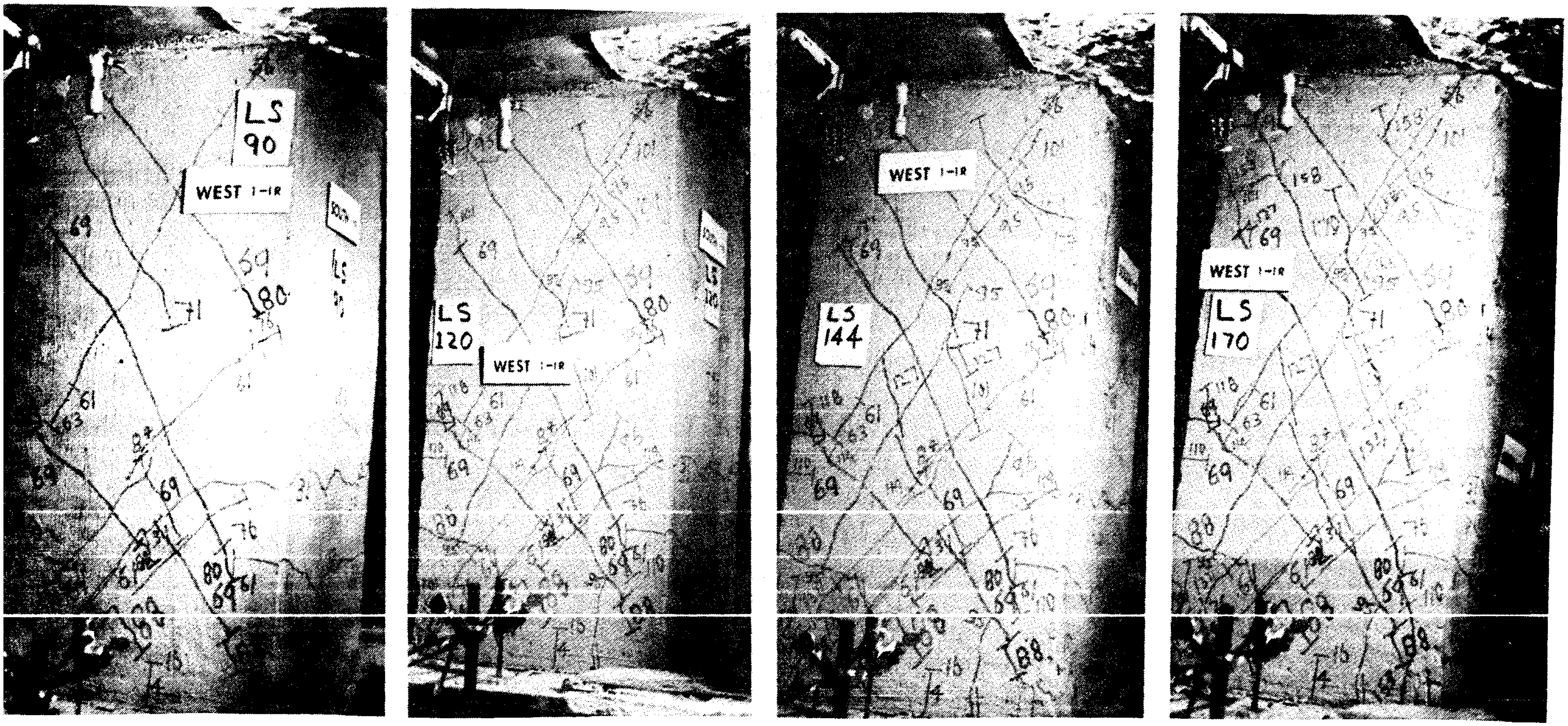

(a) 1% drift (b) 1.5% drift (c) 2.0% drift (d) 2.5% drift

Fig. 4.9 Crack patterns, Specimen 1-1R

A crude indicator of the amount of delamination between the shotcrete jacket and the original column face is the comparative hollowness of the sound produced by tapping with a hammer on the column face. All jacketed columns were investigated in this manner after testing. The east and west faces of each specimen sounded more solid than the north and south faces. Though the east and west column faces exhibited more damage as evidenced by wider and more numerous cracks, the north-south faces would be expected to indicate more delamination because of alternating extreme fiber compression and tension under north-south lateral displacements. The north and south faces of Specimen 1-3 sounded most solid, followed by those of Specimen 1-2. Specimen 1-1R had the hollowest sound.

4.2.3 Strain Distributions. Strain gages mounted on longitudinal and transverse reinforcement were monitored at each load stage for all tests. Attention was paid to the variations of strain at each drift level, and also to the history of strains at given locations under increasing drift levels.

Longitudinal Reinforcement. Figure 4.10 illustrates, as a function of peak drift levels in the north direction, the distribution of strain along the northwest #6 reinforcing bar of Specimen 1-1. Data correspond only to load stages used to produce the load-displacement envelopes of Fig. 4.5. As expected, the plot indicates the development of tension at the top of the north face, while the bottom north face of the column remains in compression. Figure 4.11 illustrates the comparable situation in Specimen 1-3. Especially noteworthy is the development of tension at both the top and bottom of the north faces as the drift level increases. This will be discussed in Chapter 5.

Longitudinal bar strains can be used to characterize the behavior of the original column section. Because the jacket longitudinal reinforcement did not extend into the end blocks, it did not develop large tension forces. Strain information from jacket bars in compression, however, can be helpful for insight into the behavior of the jacket. Figure 4.12 illustrates the history, with increasing drift levels, of strain at the top of both the #6 original column reinforcing bar and the adjacent #3 jacket reinforcing bar. For northerly displacements, the jacket bar is strained much less than the original column bar. While the jacket bar alternates between tension and compression, as would be expected from conventional beam theory, the original column bar experiences tension at the top under cycling in either direction. This was also observed in Specimens 1-2 and 1-1R, and will be discussed in Chapter 5.

Transverse Reinforcement. Figure 4.13 illustrates, for increasing drift levels, the averaged strains from the rectangular ties running in the north-south direction (east-west faces of the column) in Specimen 1-1. The mid-height tie experienced the greatest

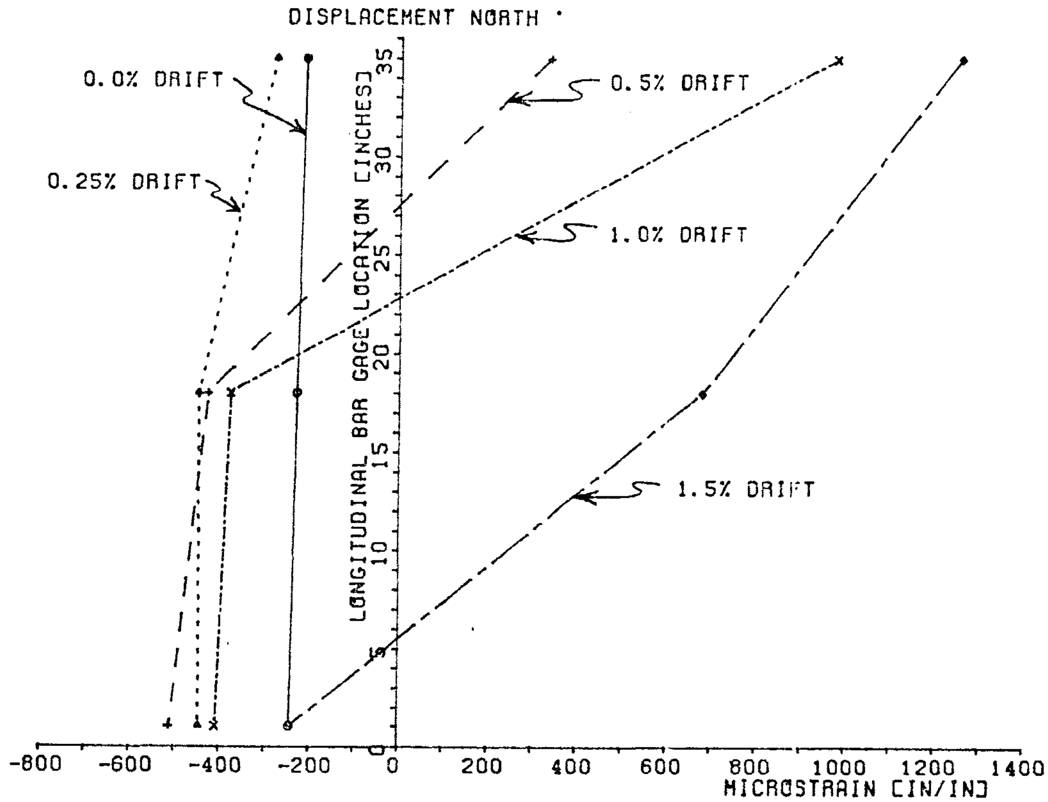

Fig. 4.10 Envelopes of strain distribution, NW longitudinal #6, Specimen 1-1

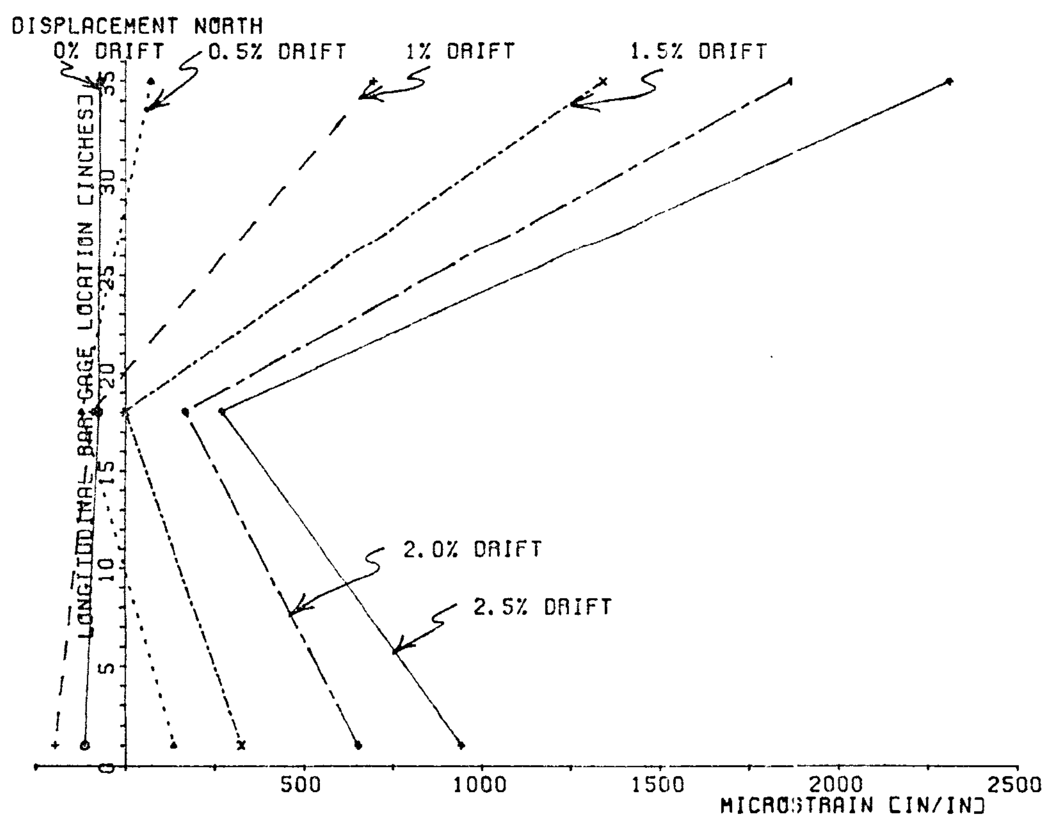

Fig. 4.11 Envelopes of strain distribution, NW longitudinal #6, Specimen 1-3

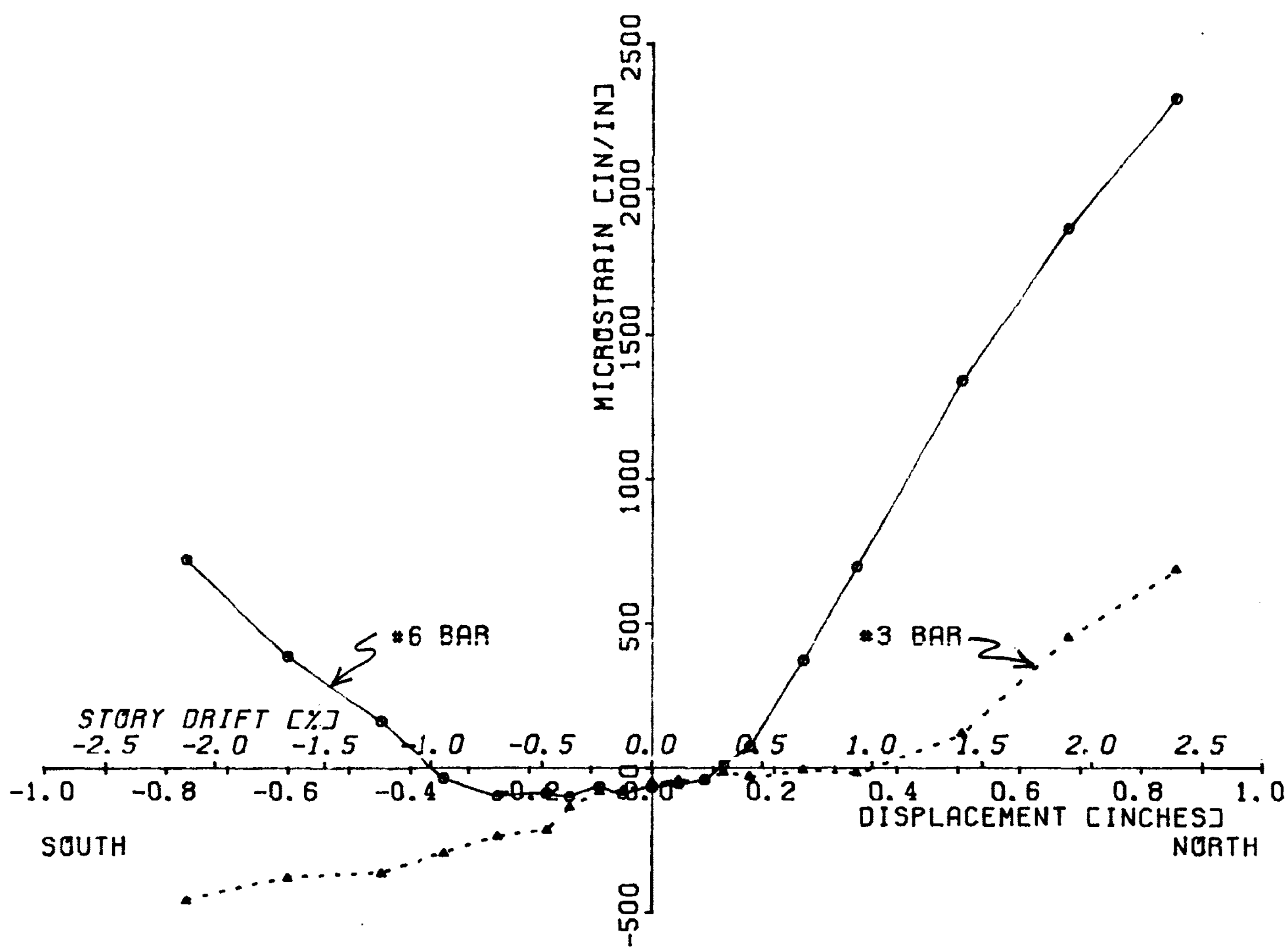

Fig. 4.12 Envelopes of top gage strain, #6/#3 NW longitudinal bars, Specimen 1-3

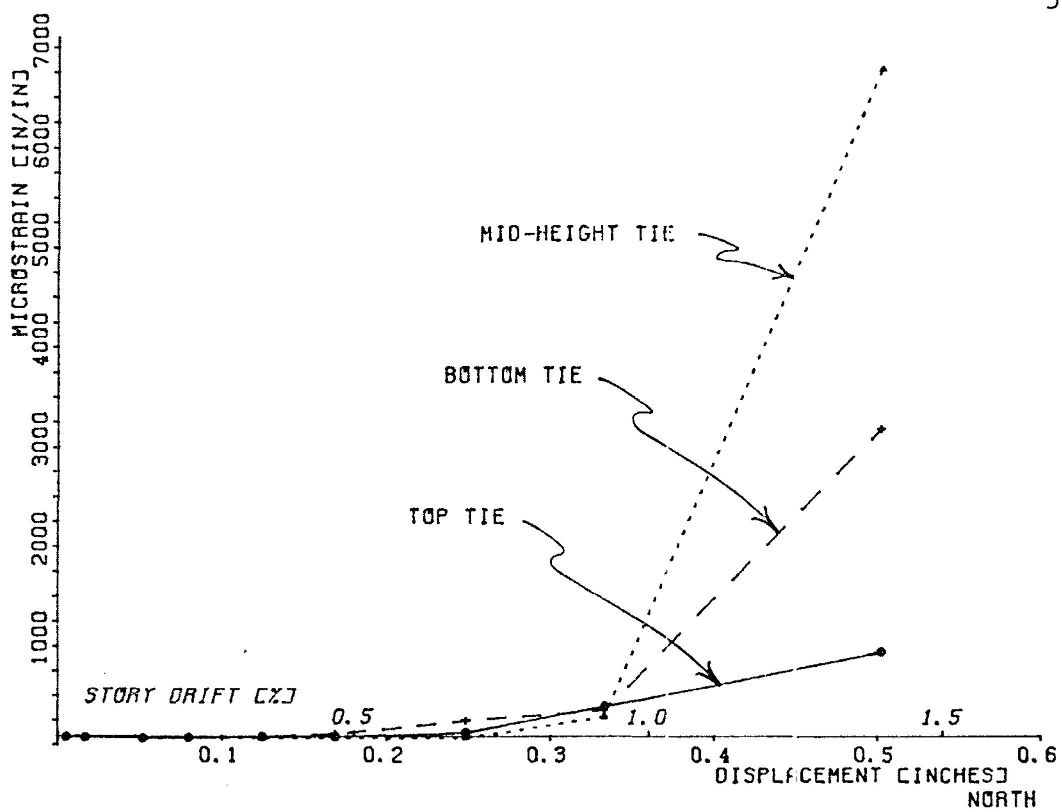

Fig. 4.13 Strain envelopes, N-S direction, original column ties, Specimen 1-1

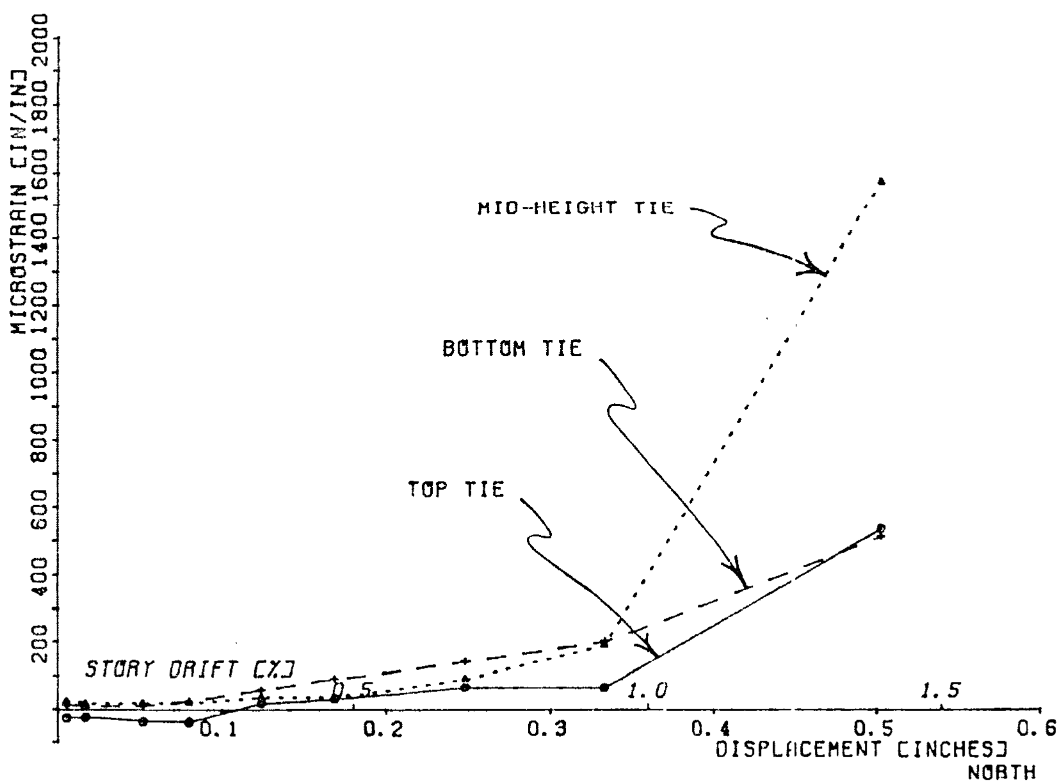

Fig. 4.14 Strain envelopes, E-W direction, original column ties, Specimen 1-1

increase in strain between the 1 and 1.5% drift levels, which also corresponds to the formation of significant inclined cracks at column mid-height (Fig. 4.6). At 1.5% drift, only the top tie remained elastic. Similarly, Fig. 4.14 illustrates the averaged strains for ties running in the east-west direction (north-south faces of the column). As before, the strain increased significantly between 1 and 1.5% drift level. Figures 4.15 and 4.16 illustrate averaged strains at mid-height of Specimens 1-1R and 1-3 for both jacket and original column rectangular ties. Gages located on east and west face ties exhibited the greatest increase in strain following the formation of inclined cracks between the 1 and 1.5% drift displacement levels. At peak displacement, only the east-west face jacket ties approached yield. Because the core was damaged before jacketing, the jacket tie strains in Specimen 1-1R were much higher at comparable drift levels than similar ties in the strengthened specimens (1-2,1-3).

Crossties. Specimens 1-3 and 1-1R had #3 crossties in both the north-south and the east-west directions. The purpose of these crossties was to provide confinement in the east-west direction and provide both confinement and shear resistance in the north-south direction. Histories of strain versus lateral displacement are shown in Figs. 4.17 through 4.20. At comparable drift levels the crossties running in the east-west direction consistently experienced less stress than those in the north-south direction because the north-south crossties had to resist shear in addition to providing confinement. A comparison of north-south crosstie strain readings for Specimens 1-3 and 1-1R indicates that crossties in the strengthened specimen (1-3) were strained about half as much as those in the repaired specimen (1-1R) at comparable drifts. The north-south crossties in both specimens developed significant strains at drifts in excess of 1 and 0.5% respectively, corresponding to the formation of inclined cracks and increasing tranverse tie strain.

4.2.4 Slip. The jacketing technique results in an interface between new and existing concrete in the strengthened and repaired specimens which affects the performance of the columns. Movement of the shotcrete jacket with respect to the original column would indicate that the cross-section was not resisting flexure monolithically, and could imply that the jacket was not fully effective in confining the original column nor in resisting shear.

Representative plots of jacket movement with respect to the original column were shown in Figs. 4.21 and 4.22 for Specimen 1-3. Positive slip corresponds to upward movement of the jacket with regard to the original column. Similar behavior was observed for all strengthened and repaired specimens. In each case, slip wire data appeared to indicate that the mid-height portion of the jacket moved upward relative to the original column at about 1% drift. The bottom portion of the jacket appeared to move downward with respect to the original column at about the same drift. This would suggest the

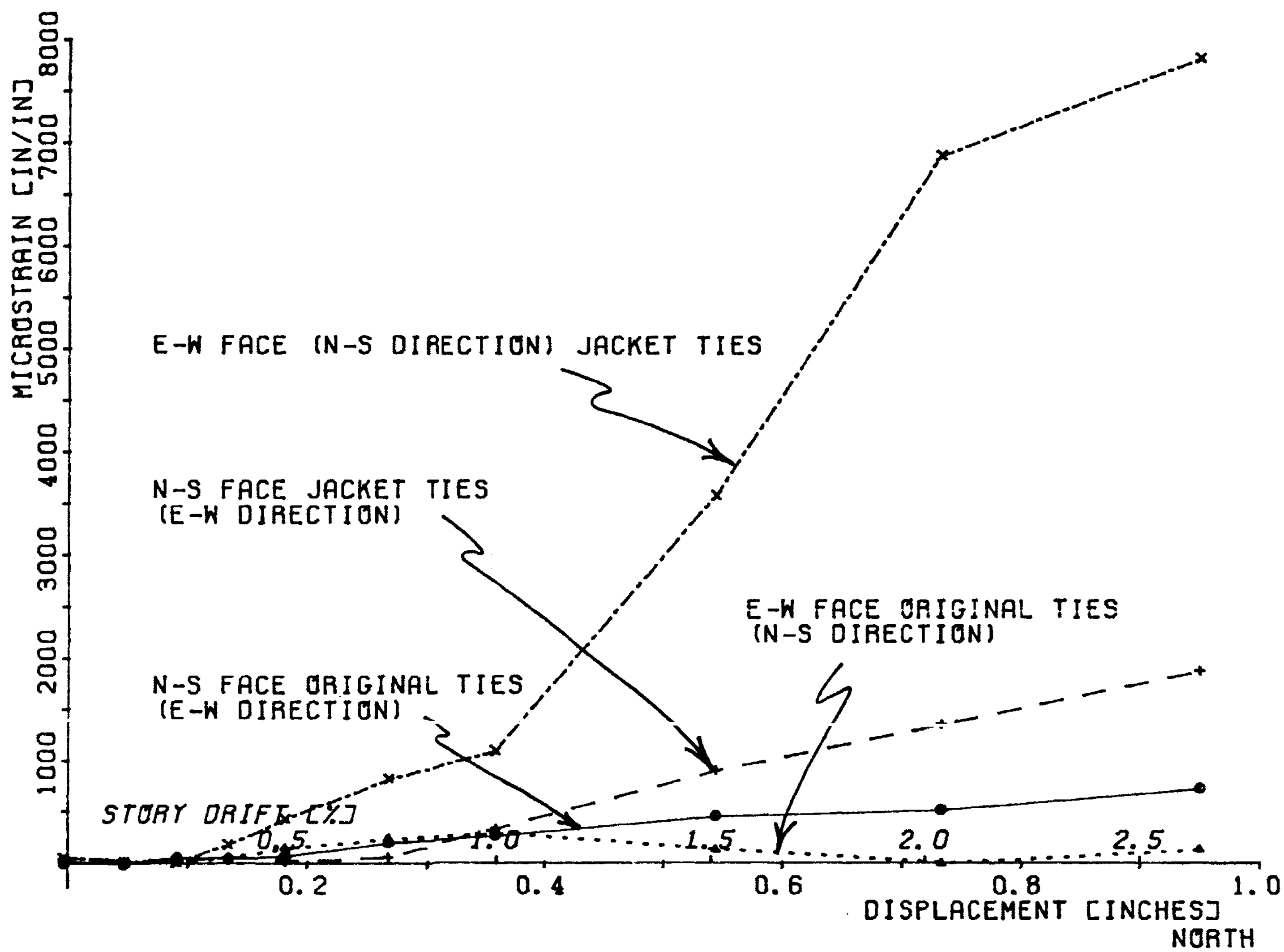

Fig. 4.15 Strain envelopes, mid-height ties, Specimen 1-1R

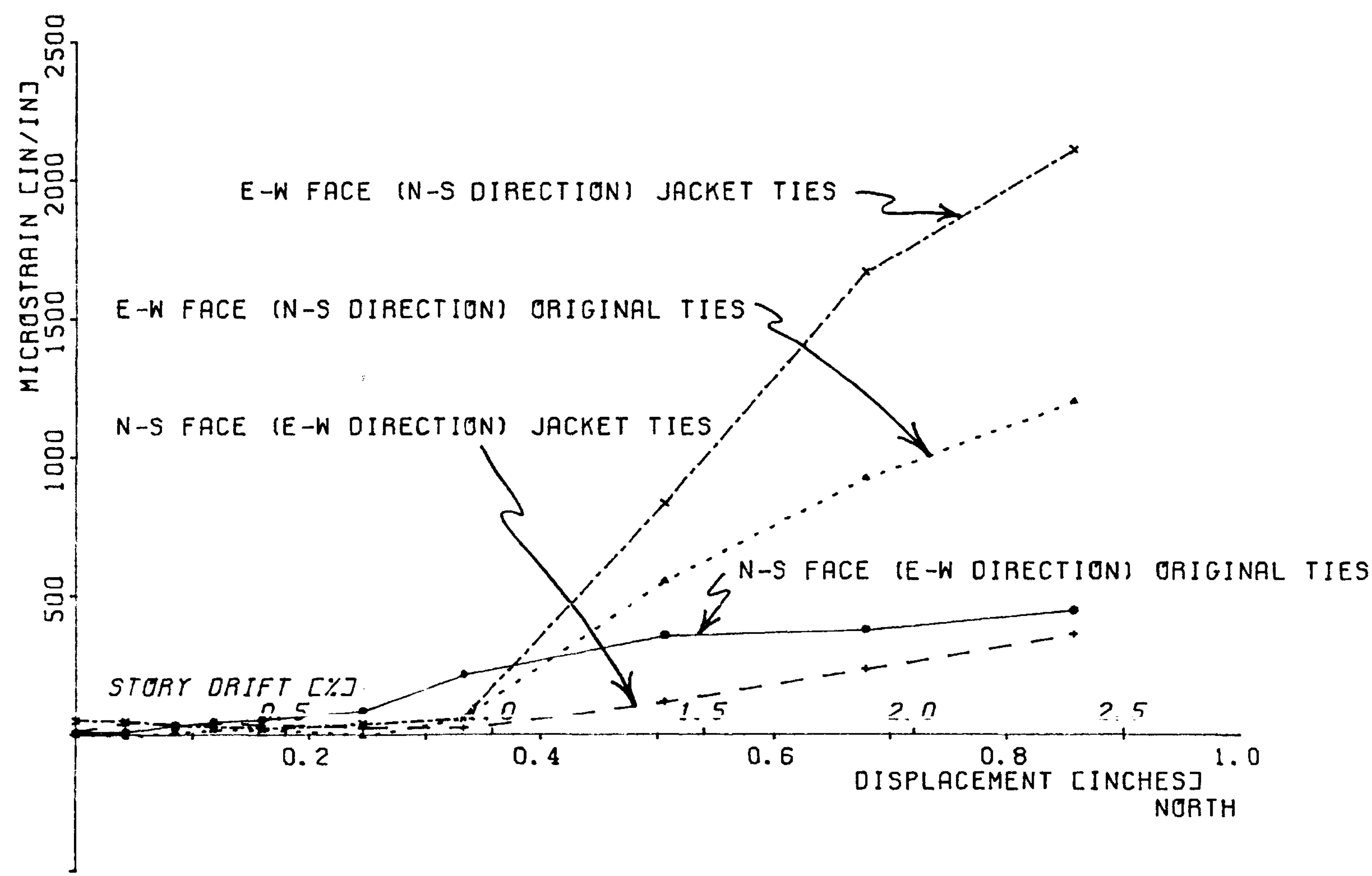

Fig. 4.16 Strain envelopes, mid-height ties, Specimen 1-3.

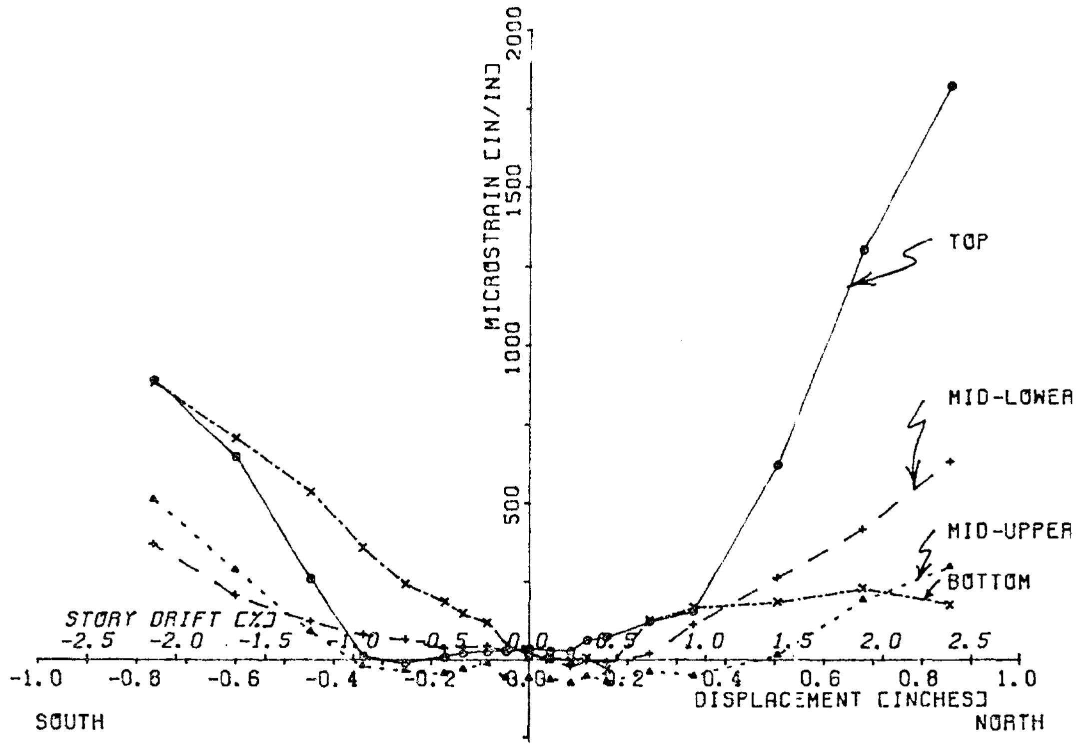

Fig. 4.17 Strain envelopes, N-S crossties, Specimen 1-3

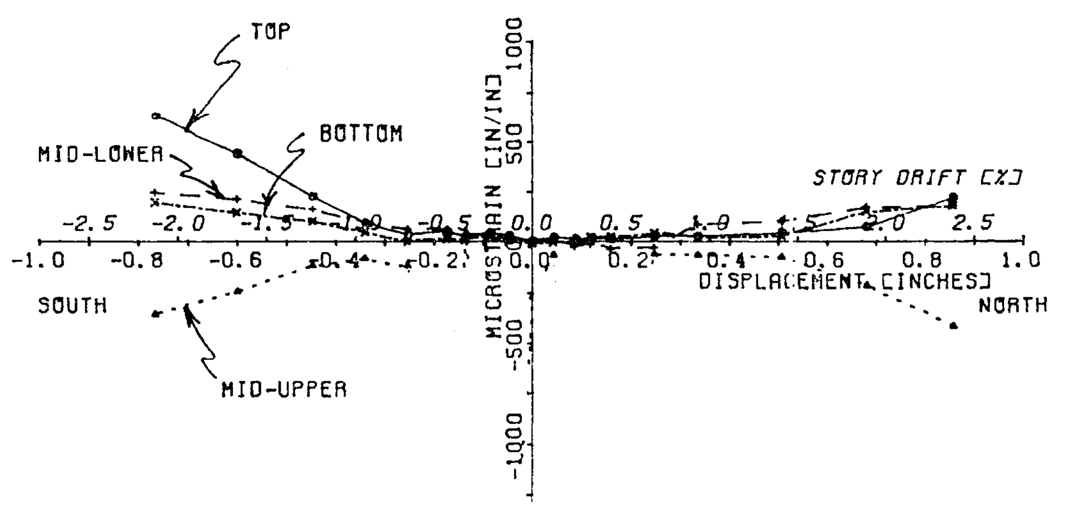

Fig. 4.18 Strain envelopes, E-W crossties, Specimen 1-3

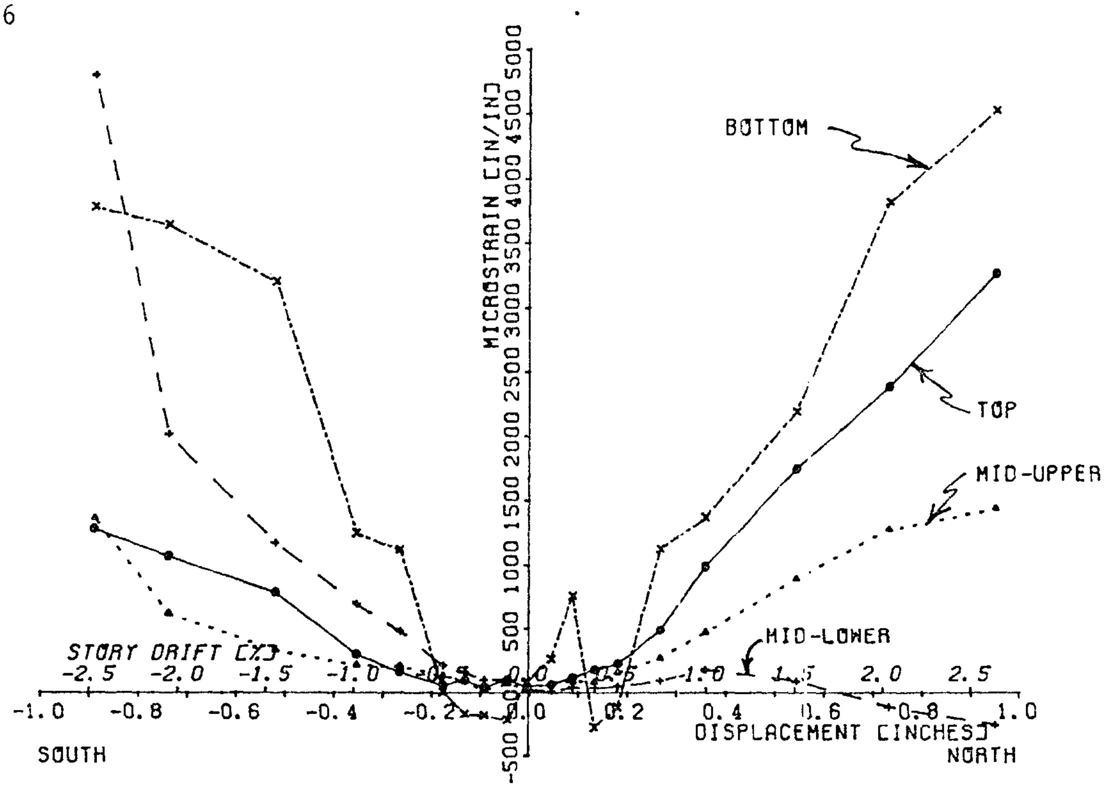

Fig. 4.19 Strain envelopes, N-S crossties

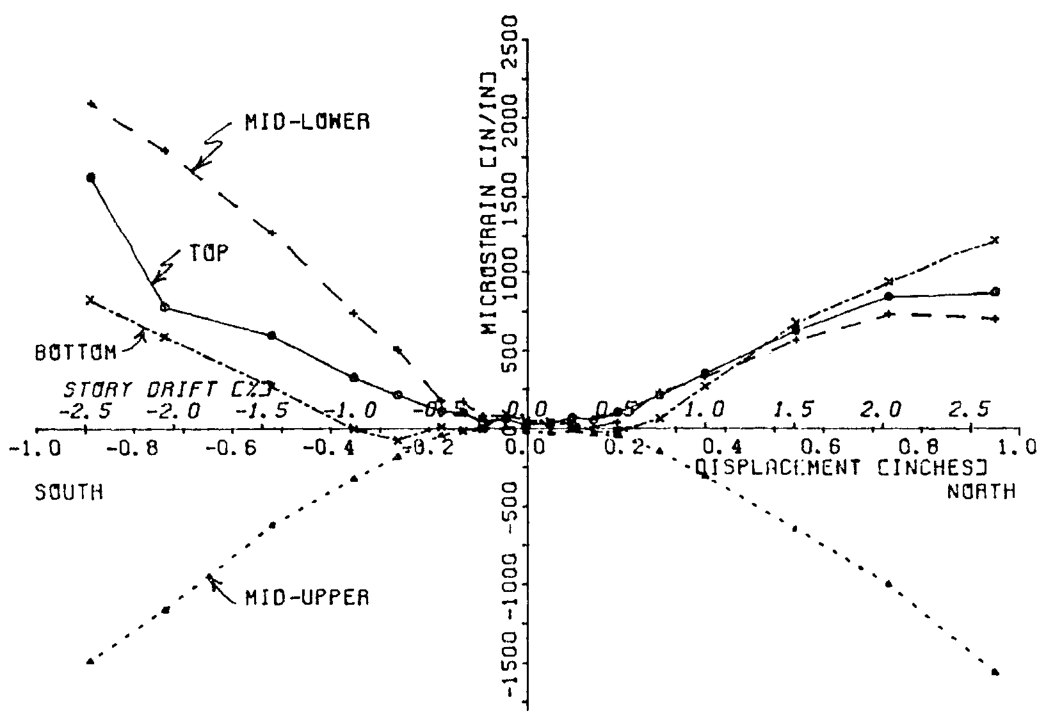

Fig. 4.20 Strain envelopes, E-W crossties

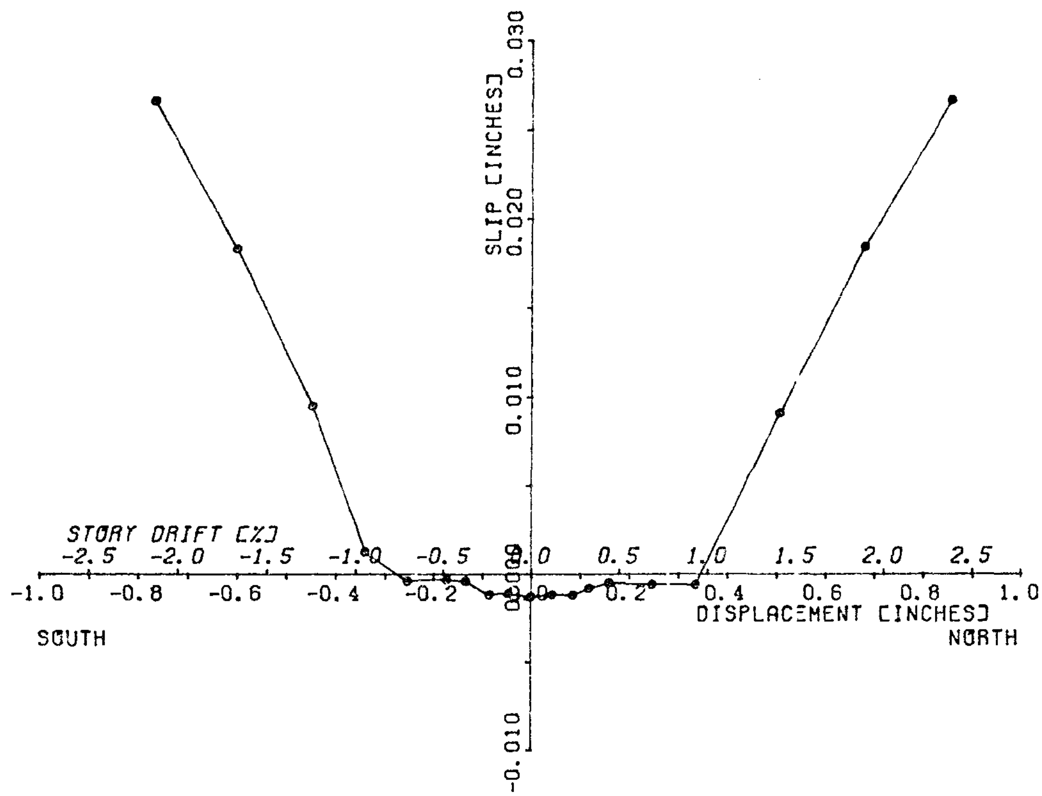

Fig. 4.21 Envelope of mid-height jacket slip, Specimen 1-3

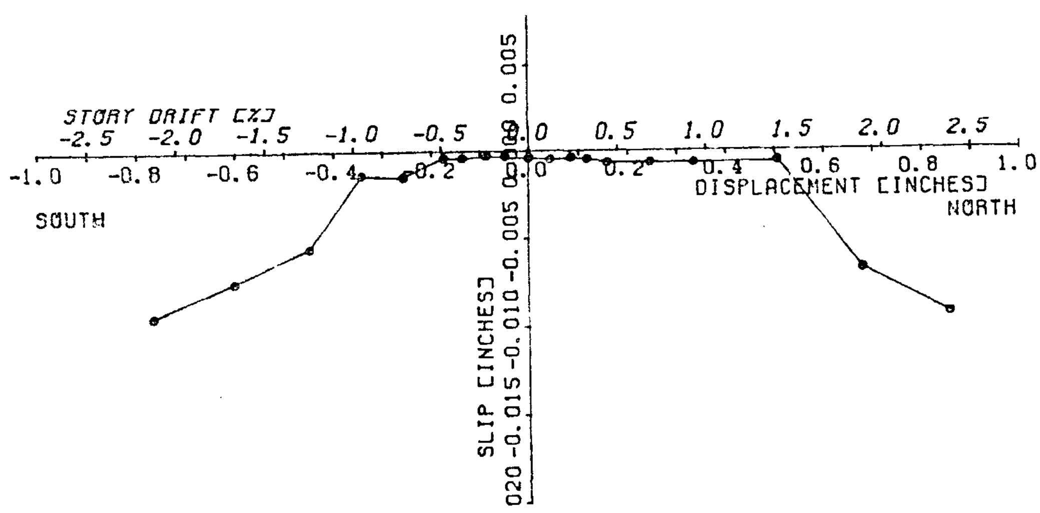

Fig. 4.22 Envelope of bottom jacket slip, Specimen 1-3

presence of significant cracks between the locations of slip wires in the shotcrete jacket. However, such cracks were not observed.

Care must be exercised in drawing conclusions based on this slip data. First, the magnitude of slip measured in all tests is at the lower limit of the sensitivity of the linear potentiometer used. Second, the linear potentiometer, mounted as shown in Fig. 3.12, could not distinguish between movement of the slip wire and outward movement of its support rod due to lateral expansion of the column. Third, slip in Specimen 1-3, whose jacket was reinforced with crossties, was about twice that of Specimens 1-2 and 1-1R. Intuitively, the crossties would be expected to inhibit relative movement between the shotcrete jacket and the original column.

CHAPTER 5

DISCUSSION OF TEST RESULTS

5.1 Introduction

In this chapter, the results of the four tests on three will be compared. The behavior of the columns will be compared in terms of load-deflection curves and strain distributions. The experimentally observed lateral capacity will be compared with computed values.

5.2 Test Results

5.2.1 Specimen Stiffness and Capacity. An indication of the relative stiffness of each specimen can be seen in Figs. 4.1 through 4.4. Unstable hysteretic behavior (pinching) is predominant in Specimen 1-1, and much less evident in the repaired or strengthened columns (Specimens 1-1R, 1-2 and 1-3). Specimen 1-1 exhibited stable hysteretic behavior for deformations up to 1% drift, but showed considerable loss of stiffness at 1.5% drift. Unstable, degrading hysteretic behavior was observed for drift levels in excess of 1.5%. The strengthened specimens (1-2 and 1-3) exhibited stable hysteretic behavior for deformations up to 1.5% drift, after which pinching and loss of stiffness became apparent. In the first cycle to each drift level, the repaired specimen (1-1R) exhibited load-deflection behavior similar to that of the strengthened specimens, but degraded much faster than the strengthened specimens under constant amplitude cycling beyond 1.5% drift. Neither the strenthened nor the repaired specimens exhibited the dramatic loss of stiffness observed in Specimen 1-1 beyond 1% drift.

The stiffness of each specimen can be compared graphically using the load-displacement envelopes of Fig. 4.5, which illustrates the improved performance of both the strengthened and repaired specimens compared to the original column (Specimen 1-1). Table 5.1 summarizes the first cycle secant stiffness (applied lateral force divided by lateral displacement) of each specimen for various drift levels. Specimens 1-2 and 1-3 had nearly equal first-cycle stiffnesses, and both were about 10% stiffer than the repaired Specimen 1-1R in this respect.

The effect of cycling on specimen stiffness can be seen in Figs. 4.1 through 4.4. The load-displacement envelopes for the first and third cycles to equal drift levels are shown for each specimen. Table 5.2 summarizes the percentage losses in secant stiffness between

TABLE 5.1 Secant Stiffness in First Cycle to Various Drift Levels

Drift Level	Secant Stiffness (kip/inch) Specimen 1-1	Specimen 1-2	Specimen 1-3	Specimen 1-1R
0.25	204	259	270	235
0.5	192	242	250	218
0.75	162	220	221	193
1.0	143	199	195	178
1.5	95	156	158	146
2.0	62	127	130	119
2.5	---	109	110	93

TABLE 5.2 Reduction in Secant Stiffness Between 1st and 3rd Cycles

Drift Level	Secant Stiffness Reduction (%) Specimen 1-1	Specimen 1-2	Specimen 1-3	Specimen 1-1R
0.5	7	7	2	5
1.0	13	7	3	7
1.5	23	8	8	9
2.0	--	7	7	11
2.5	--	11	7	12

the first and third cycles at a constant drift level. Specimens 1-1 and 1-1R experienced the greatest degradation, and Specimen 1-3 the least.

The lateral resistance of Specimen 1-1 decreased as drifts were increased beyond 1%. Other specimens did not degrade as much in this respect. The jacketed specimens exhibited increased resistance with increased drifts up to 2.5 percent.

5.2.2 Strains in Reinforcement

Longitudinal Reinforcement. Comparison of longitudinal bar strains in Specimen 1-1 (Fig. 4.10) versus those of either Specimen 1-2, 1-3 (Fig. 4.11), or 1-1R indicates that the original column had a different strain distribution from that of either the strengthened or repaired specimens. Conventional flexural theory indicates that a beam-column, subjected to equal end moments, and having a point of inflection at mid-height, will have a strain gradient ranging from tension to compression along longitudinal reinforcement. Specimen 1-1, with as aspect ratio of about 1.7, conforms to this conventional expectation. However, as mentioned in Chapter 4, plots indicate that tension develops along the entire length of the longitudinal reinforcement in both the strengthened and repaired specimens. This phenomenon can be explained in terms of two important differences between the original and the jacketed columns: 1) the location of the neutral axis; and 2) the effects of diagonal tension on the internal resisting moment within the column.

Prior to the formation of inclined cracks, and assuming little bond deterioration, longitudinal steel strains are consistent with the predictions of simple bending theory. Analysis using the computer program RCCOLA [15] indicated that regardless of moment direction, the position of the jacketed column's neutral axis placed all of the original column longitudinal reinforcement in tension. Figure 5.1(a) illustrates the effect of this neutral axis location on strains within a single longitudinal bar. The bottom portion of the bar is in tension even though it is located on the "compression" face of the column.

Paulay, in his study of coupling beams [22] has shown that due to the effects of diagonal tension, flexural members with shear span/depth ratios less than about two have tensile stresses along the entire length of their longitudinal reinforcement, even at locations where conventional flexural theory would predict compressive stresses. Such a distribution is shown in Fig. 5.1(b) and becomes more dominant with decreasing shear span/depth ratios. The addition of the shotcrete jacket to the original column deepens the section, resulting in a coupling beam effect.

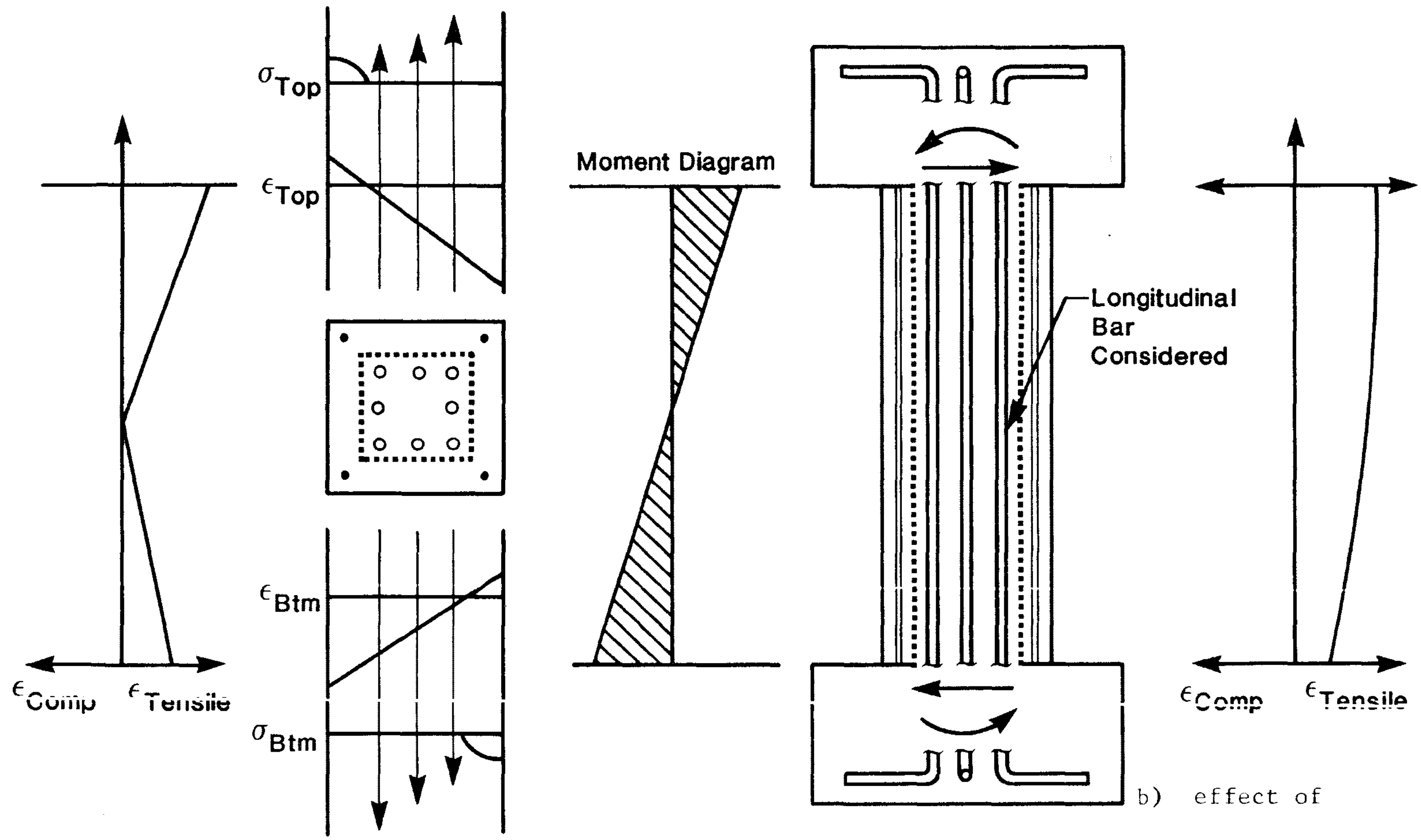

a) effect of neutral axis location

b) effect of diagonal tension

Fig. 5.1 Predicted envelopes of longitudinal bar strains

In all strengthened and repaired specimens, both effects were observed. The position of the neutral axis influenced bar stresses from the start of the tests, and the effects of diagonal tension increased as the tests proceeded. Figure 4.9 shows the shift of the strain envelope from one resembling Fig. 5.1(a) to one resembling Fig. 5.1(b) at 1.5% drift. Subsequent larger drifts lengthened the inclined cracks, shifting the strain envelope even more.

The jacket longitudinal reinforcement was not continuous into the end blocks of the specimens. It serves to hold the jacket transverse steel during construction but makes no contribution to the section capacity. Both the strengthened and repaired specimens exhibited similar behavior in both the original column and jacket reinforcement. Strains in the original longitudinal reinforcement typically started to increase at about 0.5% drift, with relatively large increases occurring with increasing drift. On the other hand, strains in longitudinal jacket reinforcement increased much more slowly with increasing drift for all specimens. For large drift values in the northerly direction, when the reinforcement at the top north face of both the original column and the jacket was in tension, the jacket reinforcement had little strain. At similar displacement levels, the jacket reinforcement in Specimen 1-1R exhibited higher strains. This appears reasonable, because the core of Specimen 1-1R had been badly damaged by the first test, the shotcrete jacket had to carry a larger share of the imposed forces. However, the jacket longitudinal reinforcement in all specimens did not develop significant tension.

<u>Tranverse Reinforcement</u>. Distribution of shear between concrete and steel, and relative confining effects of transverse steel were investigated using strain gages mounted on the transverse reinforcement in both the jacket and the original column. Transverse reinforcement on the east and west faces of the column resisted north and south loads, and confined the concrete core. All strengthened specimens exhibited similar behavior in that drifts in excess of 1% caused large increases in strain in transverse reinforcement on the east and west faces (north-south direction). In all specimens, this drift level also corresponded to the formation of inclined cracks at column mid-height.

Up to drifts of 2%, little if any yielding occurred in the transverse steel of the strengthened specimens. However, this was not the case for the repaired specimen. Inspection of transverse tie strain data for Specimens 1-3 and 1-1R indicates that the jacket transverse reinforcement in the north-south direction yielded before 2% drift, and reached strains far in excess of those recorded for the jacket ties in the strengthened specimens. This is reasonable considering that the original column core of this specimen was badly damaged in the first test, and the original column ties were therefore not fully effective.

Transverse reinforcement on the north and south faces (east-west direction) confined the column core. Strains in the north and south face transverse reinforcement in both the jacket and the original column were less than yield for all specimens.

5.3 Comparison of Observed and Computed Capacity

The experimentally observed lateral capacity of each specimen was determined using: 1) load-displacement curves; 2) longitudinal steel strains in the original column; 3) curves of strains in transverse reinforcement; and 4) observations of the extent of inclined cracking.

The original column (Specimen 1-1) was analyzed as described in Section 2.3.3 using the computer program RCCOLA [15]. The program, assuming plane sections remain plane, analyzed a slice of column cross section and computed the column's flexural and shear capacity as shown in Fig. 2.2. As mentioned previously, the moment-axial force curve as governed by shear capacity is based on University of Texas short column tests [23] rather than conventional ACI [17] equations. Analyses indicated that a shear failure was likely because the predicted capacity in shear was less than that in flexure. Specimen 1-1 did have a shear-dominated brittle failure starting at about 1% drift. Longitudinal steel strains at failure were less than yield, and degradation of stiffness under cycling occurred after the transverse reinforcement yielded. The computed and observed capacities are shown in Table 5.3.

TABLE 5.3 Lateral Capacity

Specimen	Computed Lateral Capacity (kips)			Exper. Observed Capacity	Drift (%)	Computed/ Observed	
	Flexure	Shear (UT)	Shear (ACI)	(kips)		(UT)	(ACI)
1-1	64	40	31	47	1	0.85	0.66
1-2	104	100	72	90	2	1.11	0.80
1-3	104	100	72	88	2	1.14	0.82
1-1R	104	100	72	86	2	1.16	0.84

Inspection of Table 5.3 reveals that the ACI shear equations (11-6, 11-7 and 11-17) consistently underestimated the section shear capacity when compared to the results of the empirical relationship discussed in Section 2.3.3.

The strengthened specimens (1-2, (1-3) were analyzed using the same program (Section 2.6.2) used for the original column. A number of additional assumptions were made in modelling the original column-shotcrete jacket combination:

1) No slip was assumed between the original column and the shotcrete jacket. The effect of relative slip would be a smaller predicted capacity based on less than monolithic action;

2) Jacket longitudinal reinforcement was assumed not to carry any tensile stress. As shown in Fig. 4.10, a small amount of tension due to bond did develop in the jacket longitudinal reinforcement, and this could be expected to increase the predicted capacity; and

3) The shotcrete jacket was assumed to be fully effective in compression. The presence of 1/64 in. shrinkage cracks at each end block would indicate less than full jacket effectiveness at low displacement levels.

The results of the analysis, shown in Fig. 2.7 and Table 5.3, indicated that the computed capacity in shear was nearly equal to that in flexure. A combination flexure-shear failure mode would be expected, considering the location of the neutral axis developed in the anaysis. Specimens 1-2 and 1-3 had flexurally-dominated failures, as evidenced by longitudinal reinforcement strains exceeding yield. Some degradation of stiffness occurred under cycling at larger drifts.

The computed flexural and shear capacities of the repaired specimen (1-1R) were nearly equal and a combined shear and flexure failure could be expected. Specimen 1-1R did exhibit a combination shear-flexure failure, as evidenced by longitudinal steel strains slightly less than yield at peak displacements, significant degradation of stiffness under cycling, and by strains greater than yield in transverse reinforcement. Inclined shear cracks were far more numerous and wider in Specimens 1-1 and 1-1R than in either Specimens 1-2 or 1-3.

In summary, for the strengthened and repaired specimens, experimentally observed lateral capacity was about 10 to 15% less than that computed using ACI equations and about 10% more than that using empirical equations developed expressly for short columns.

CHAPTER 6

SUMMARY AND CONCLUSIONS

6.1 Summary of Investigation

The behavior of strengthened and/or repaired reinforced concrete short columns under cyclic deformations was studied. The primary objective of the study was to evaluate the effectiveness of various techniques for strengthening or repairing short columns.

Based on an 18-in. square prototype column, three column test specimens were constructed to two-thirds scale, using identical geometry and reinforcement. The original specimens had a 12-in. square cross section reinforced with eight #6 longitudinal bars, sets of 6 mm ties spaced at 8 in., and 1 in. cover. Spacing of the transverse reinforcement, though greater than what would currently be specified, was intended to represent the practice of column design in seismic regions of the U.S. in the 1950's and 1960's.

One of the original specimens was tested (Specimen 1-1), repaired, then retested (Specimen 1-1R). Repair of that specimen consisted of removing loose cover, adding #3 longitudinal bars at each corner, epoxying #3 crossties in each direction at 9 in., hooked around a #6 mid-face bar, and adding 6 mm deformed transverse ties at 2.5-in. spacing. The damaged column was then encased with a 2.5 in. shotcrete jacket which provided a 1-in. cover over the added reinforcement, resulting in a 17 in. square column. The remaining two specimens (Specimens 1-2 and 1-3) were strengthened prior to testing. Specimen 1-2 was strengthened by adding #3 longitudinal bars at each corner, 6 mm ties at 2.5 in., and a 2.5 in. shotcrete jacket, resulting in 1 in. clear cover and a 17 in. square column. Specimen 1-3 was strengthened similarly to the repaired specimen (1-1R) using #3 longitudinal bars at each corner, 6 mm ties at 2.5 in., plus crossties hooked around #6 longitudinal bars at mid-face.

The specimens were loaded laterally using an apparatus designed to permit movement of one column end while preventing rotations of both ends. A single displacement history was used for all tests. Typically, each specimen was subjected to three reversed cycles of lateral displacement to drifts of 0.5, 1.0, 1.5, 2.0, and 2.5%. A constant axial load of 64.8 kips was applied in all tests. During each test, measurements were taken at each load stage to determine the applied forces, lateral deflection, and strains in the longitudinal and transverse reinforcement. Fixity of the column ends was also monitored. Cracks were marked at each peak deflection.

6.2 Summary of Test Results

6.2.1 Original Column Specimen. Specimen 1-1 exhibited stable hysteretic behavior for deformations up to 1% drift after which considerable loss of specimen stiffness occurred under cycling. Failure appeared to be dominated by shear, as evidenced by pinching of the hysteretic loops, and the development of longitudinal reinforcement strains significantly less than yield. Extensive inclined cracks developed at 1% drift and steadily lengthened with cycling. Analyses indicated that the original column shear capacity was significantly less than flexural capacity and a brittle shear failure was predicted. The original column specimen behaved satisfactorily at drift levels less than 0.5% where response was essentially elastic. However, its loss of strength and stiffness at larger drifts indicated that the original specimen could not provide adequate cyclic lateral resistance in the inelastic range.

6.2.2 Strengthened and Repaired Specimens. The strengthened and repaired specimens were designed to fail in a more ductile manner than the original column. Analysis of the strengthened specimens indicated a combination flexure-shear failure (shear capacity was about equal to its flexural capacity). The shotcrete jacket was assumed to behave integrally with the original column and improve inelastic strength and stiffness due to the confining interaction of the transverse and longitudinal steel.

Both the strengthened and the repaired columns exhibited greater ductility than the original column. Both strengthened specimens (Specimen 1-2 and 1-3) exhibited similar load-deflection behavior, having stable hysteretic loops for deformations up to 1.5% drift, after which loss of stiffness became apparent. Failure appeared to be flexurally dominated, as evidenced by the development of strains in excess of yield in the original column longitudinal reinforcement. Jacketing both with and without supplementary crossties resulted in much greater stiffness and strength than that of the original, unstrengthened specimen. Inclined cracks developed in both strengthened specimens at drifts in excess of 1%, coinciding with increases in measured strains in the transverse reinforcement. Supplementary crossties did not significantly increase specimen strength nor stiffness in the first cycle to a given drift level, but were beneficial in delaying strength and stiffness deterioration under repeated cycles to drift levels exceeding 2%.

The repaired specimen (1-1R) exhibited stable hysteretic behavior for deformations up to 1.5%, after which it began to lose stiffness under cycling. Failure appeared to be a combination of shear and flexure, as evidenced by yield of the original column longitudinal reinforcement, coinciding with pinching of the hysteretic loops.

The repaired specimen had much greater lateral stiffness and strength than the original specimen, and about 10% less than the strengthened specimens at the first cycle to a given drift level. Inclined cracks developed in the repaired specimen at 1% drift, coinciding with increases in measured strains in the transverse ties and crossties which was in excess of yield at large drifts. Inclined cracks were longer, wider, and more numerous in the repaired specimen than in either of the strengthened specimens. The repaired specimen degraded much faster than either of the strengthened specimens under repeated cycles to drift levels exceeding 2%.

6.3 Conclusions

1) A two-thirds scale model of a typical column designed for seismic areas in the 1950's and 1960's performed poorly under reversed cyclic lateral deformations exceeding 0.5% drift. As indicated by analysis, the column shear span/depth ratio and reinforcing details resulted in a brittle, shear-dominated failure. This situation can be remedied either by strengthening the columns to produce a more ductile member, as described here, or by providing additional elastic capacity in the form of shear walls or bracing.

2) A number of techniques can be used to strengthen existing columns in order to improve their performance under reversed lateral deformations. In this study, encasement of the original square column with a shotcrete jacket reinforced with corner longitudinal bars and closely-spaced ties significantly increased its stiffness and lateral capacity. Care was taken to develop a column whose failure would be ductile at the reduced shear span/depth ratio caused by jacketing. A 2-1/2 in. spacing of jacket transverse reinforcement provided increased confinement and shear resistance, and was not hard to fabricate. An upper bound to the lateral capacity of the strengthened column was calculated assuming integral behavior of the shotcrete jacket and the original column. Shear capacity was predicted using equations developed from tests of short columns. ACI equations consistently underestimated the shear capacity.

3) The strengthening technique described above was varied in one specimen to increase the confinement provided by the jacket. Additional midface longitudinal bars were placed in the jacket, and connected by crossties grouted with epoxy through the original column. This modification did not significantly effect the monotonic stiffness or strength but did decrease the rate of strength and stiffness degradation under repeated cycles of reversed lateral displacements exceeding 2% drift.

4) When a badly damaged column was repaired by encasing the core with a shotcrete jacket reinforced with closely-spaced ties, and with crossties connected to midface longitudinal bars, the strength and stiffness were nearly equal to those of an undamaged column strengthened with the same jacket. The crossties and midface bars contributed significantly to the confining effect of the jacket transverse reinforcement.

6.4 Additional Research

Based on the results of the current investigation, the following future research is suggested:

1) Study is needed regarding the effects of varying the proportions of both the column and the jacket. The performance of a strengthened section may differ considerably depending on the relative proportions of the added jacket to the original column.

2) The effect of epoxy injection of cracks in a damaged column needs study. Repair of the original column core may reduce the deterioration of strength and stiffness when the is cycled repeatedly to large drift levels.

N O T A T I O N

a Shear span, in.

A_c Area of concrete core, out-to-out of ties, in.^{2}

A_g Gross area of cross section, in.^{2}

d Distance from extreme compression fiber to the centroid of the tension reinforcement, in.

d^* Distance from extreme compression fiber to the centroid of the extreme tension reinforcement, in.

E Modulus of elasticity of reinforcement

E_{STH} Modulus of elasticity of reinforcement at the onset of strain hardening

f'_c Concrete compressive strength (6 x 12 in. cylinder), psi (28 day strength for design. Strength at age of test specimen for analysis of data)

f_u Ultimate tensile strength of reinforcement

f_y Yield strength of reinforcement

N Applied axial compression, lbs.

V_{nR} Nominal shear strength of short columns, lbs

ε_{STH} Tensile reinforcement strain at onset of strain hardening

ε_u Ultimate tensile reinforcement strain

REFERENCES

1. Hanson, R. D., "Repair, Strengthening and Rehabilitation of Buildings--Recommendations for Research," University of Michigan, Report No. UMEE 77R4, October 1977.

2. Hanson, R. D., "Repair and Strengthening of Reinforced Concrete Members and Buildings," Proceedings, Workshop on Earthquake Resistant Reinforced Concrete Building Construction, University of California, Berkeley, July 1977.

3. Sugano, S., "Aseismic Strengthening of Existing Reinforced Concrete Buildings," Seminar, Seismology and Earthquake Engineering, International Institute of Seismology and Earthquake Engineering, Building Research Institute, Japan, March 1980.

4. "Guideline for Seismic Retrofitting (Strengthening, Toughening and/or Stiffening) Design of Existing Reinforced Concrete Buildings," Ministry of Construction, Japan, March 1977 (translated into English, 1980).

5. Jirsa, J. O., Maruyama, K., and Ramirez, H., "Development of Loading System and Initial Tests--Short Columns under Bidirectional Loading," CESRL Report No. 78-2, Civil Engineering Structures Research Laboratory, The University of Texas at Austin, September 1978.

6. Jirsa, J. O., Maruyama, K., and Ramirez, H., "Short RC Columns under Bidirectional Load Histories," Journal of Structural Engineering, ASCE, Vol. 110, No. 1, Paper 18511, January 1984, pp. 120-137.

7. Ramirez, H., and Jirsa, J. O., "Effect of Axial Load on Shear Behavior of Short RC Columns under Cyclic Lateral Deformations," PMFSEL Report No. 80-1, The University of Texas at Austin, June 1980.

8. Woodward, K. A., and Jirsa, J. O., "Influence of Reinforcement on RC Short Column Lateral Resistance," Journal of Structural Engineering, ASCE, Vol. 110, No. 1, Paper 18513, January 1984, pp. 90-104.

9. Moore, M. E., "Shear Strength and Deterioration of Short Lightweight Reinforced Concrete Columns under Cyclic Deformations," unpublished Master's thesis, The University of Texas at Austin, May 1982.